Volcano-stratigraphy of the extension-related silicic volcanism of the Çubukludağ Graben, western Turkey: an example of generation of pyroclastic density currents

ZEKIYE KARACIK* & SENGUL C. GENÇ

Istanbul Technical University, Faculty of Mines, Geology Department, Maslak Istanbul 34469, Turkey

Abstract – Western Turkey's extension-related Cumaovası volcanic rocks (Lower Miocene, 17 Ma) are excellent examples of silicic eruptions. The sub-aerial silicic volcanism at Çubukludağ Graben between İzmir and Kuşadası in west–central Anatolia is mainly in the form of rhyolite domes, lava flows and pyroclastic deposits. The initial features of volcanism derived from phreatomagmatic explosive eruptions from silicic magma that came into contact with lake waters during Neogene times. Most of the volcanic succession represents pyroclastic density currents (PDCs), known as the Kuner ignimbrite. The deposits are fine grained and laminated at the base and pass laterally and vertically into deposits displaying well-developed traction structures, soft sediment deformation and/or erosion channels in the NE part of the region. Alternate deposits of massive, diffusely stratified lapilli and ash are the main products of the later explosive stage. Massive lithic breccias forming the top of the sequences are the proximal facies of the PDCs. The lava phase mainly consists of rhyolite extruded as dome and fissure eruptions of lavas, aligned along NE–SW-trending faults as well as from extensional cracks that are nearly perpendicular to the main graben faults. Considering the tectono-stratigraphical aspects and geochemical nature of the study area, we propose that the Cumaovası silicic volcanism was produced by extension-related crustal melting during the Late–Early Miocene period (17 Ma).

Keywords: ignimbrite, pyroclastic density current, silicic dome, Western Turkey.

1. Introduction

Silicic magmatism is often associated with caldera-forming events that indicate rapid eruption from shallow magma chambers. Other types of magmatism are characterized by silicic domes, lava flows and associated small-volume pyroclastic deposits from single, large but shallow magma chambers over time intervals of hundreds of thousands of years. In this case, the magma chamber vents along faults before a caldera-forming eruption.

The well-studied Coso volcanic field (California, USA), the Taylor Creek rhyolite and Bearhead rhyolite (Rio Grande rift, USA) are good examples of this type of silicic system (Justet & Spell, 2001). All these rhyolite magmas are located in regional extension zones, derived or vented from extension-related faults. Large, shallow, volatile-charged silicic magma chambers produce small-scale effusive deposits and widespread rhyolitic domes in these regions.

Despite the abundance of basaltic maar volcanoes, silicic hydrovolcanic deposits and tuff rings are very rarely described in academic literature (Tait *et al.* 2009). The general form of such hydromagmatic products includes tuff rings and/or tuff cones with circular or non-circular morphologies created as a result of the eruption style and vent conditions. Lateral vent migration resulting from the collapse of an unstable sedimentary substrate (e.g. Jeju Island, Korea) controls

the volcano-morphology and structures (cf. Sohn & Park, 2005).

We have undertaken a field-based study focusing on the genetic relationship between volcanic centres and fault types in the important tectonic transfer zone of the NE–SW-trending Cumaovası volcanic belt of Western Anatolia (Fig. 1). There have been only a few previous studies on Cumaovası silicic volcanism and these have been based on limited geochemical and geochronological data (Borsi *et al*. 1972; Innocenti & Mazzuoli, 1972). The magmatic nature, petrogenetic evolution and radiometric ages of Cumaovası silicic volcanic rocks and their relationship with Western Anatolian Neogene volcanism has been discussed recently by Karacık *et al.* (2013). They proposed that the rhyolitic lavas of the Cumaovası volcanic rocks were generated from crustal melting caused by extension-related mafic inputs into the upper crust. This would have given the rhyolitic lavas a unique chemical composition, similar to extension-related rhyolites formed from small magma bodies.

The Neogene volcanism of Western Anatolia started at *c.* 20 Ma with intermediate volcanic products and was followed by bimodal, basic and silicic lavas between 17 and 15 Ma (Helvacı *et al.* 2009; Karacık *et al*. 2013). Typical volcanic products of this period mainly crop up in the Karaburun Peninsula, Foça and Dikili regions (Fig. 1). The Cumaovası volcanic rocks which occur in the NE–SW-trending Çubukludağ Graben are the silicic member of this bimodal volcanism (Genç *et al.* 2001; Uzel & Sözbilir, 2008; Karacık
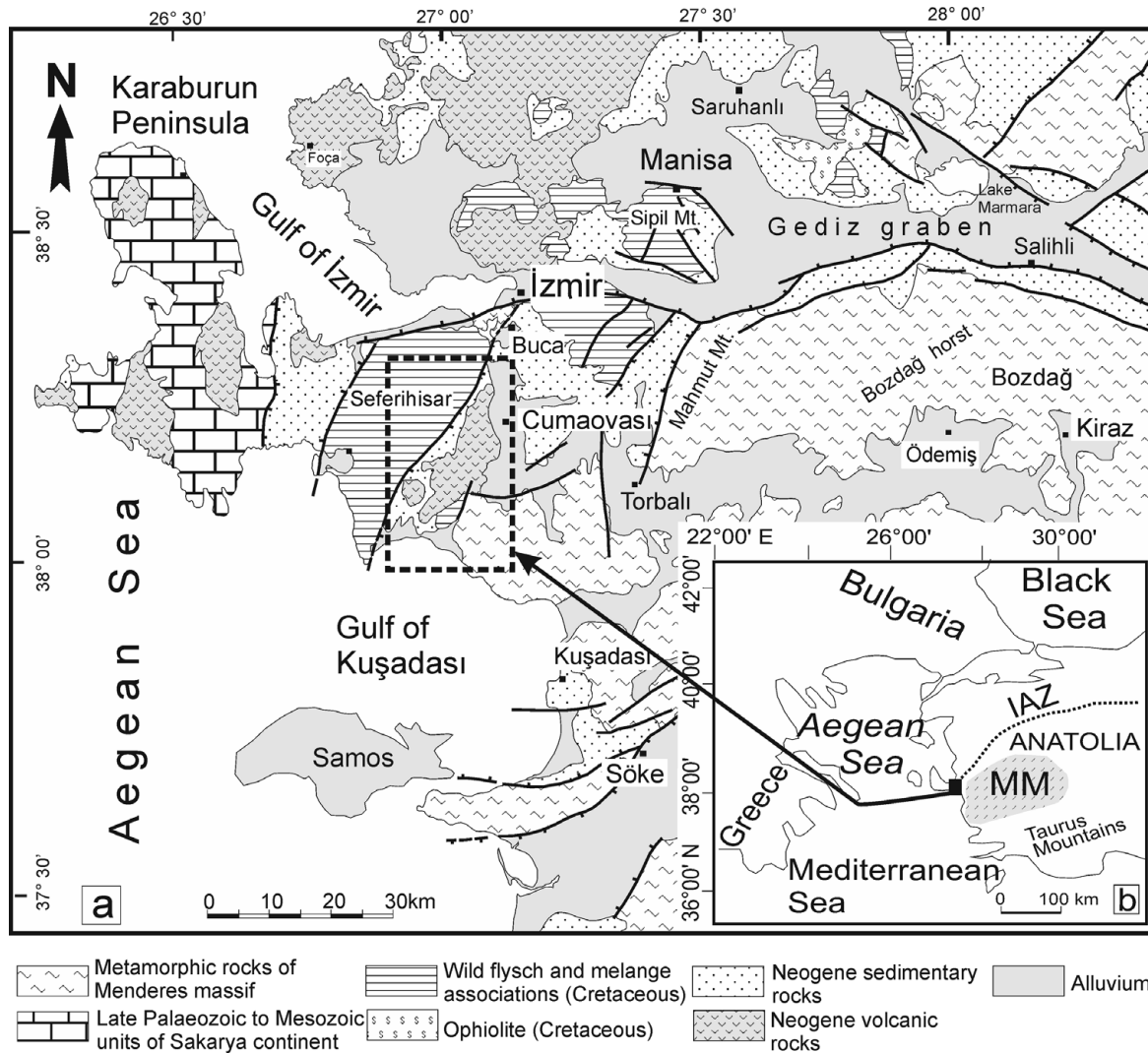
*Author for correspondence: zkaracik@itu.edu.tr

Figure 1. Simplified geology map of the central Western Anatolia (modified from Genç *et al.* 2001). Inset map indicates Aegean region major tectonic features. IAZ – Izmir Ankara Suture zone; MM – Menderes massif. See the online Supplementary Material at http://journals.cambridge.org/geo for a full colour version of this figure.

et al. 2013) (Figs 1, 2). The WNW and ESE margins of the Çubukludağ Graben are identified by oblique-slip faults, controlling the sediment deposition in the basin. Our field studies revealed that a clear genetic relationship exists between volcanism, sedimentation and fault systems. Tectono-magmatic relationships also show that rhyolitic centres were associated with normal faults. The highly viscous rhyolite magma eruptions appear to have been facilitated by the tectonic extension.

The Cumaovası volcanism consists mainly of silicic explosive and effusive units. The main products of this volcanic succession are rhyolitic lavas which form different-sized domes, fissure eruptions and related pyroclastic deposits. Our data and analysis show a gradual transition from sedimentary to pyroclastic units north of the Çubukludağ Graben. Detailed mapping of these volcanic features and measurements from nine stratigraphic sections have been collected in order to determine the nature of pyroclastic activity and their products.

Our study explains the volcanic history and dynamics of the Neogene and the extension-related silicic

system of the Western Anatolia, and compares these with silicic volcanic products from other extensional regions.

2. Geological setting

The NE–SW-trending Çubukludağ Graben is located between the İzmir and Kuşadası regions in Western Anatolia (Turkey). It lies between the Aegean coastline in the south and the Cumaovası plain to the north (Fig. 1). The area is dominated by two E–W-trending fault zones in the north and south, which controlled the E–W-trending Gediz Graben and Kuşadası Basin, respectively (Fig. 1). In the Çubukludağ region there are two major rock groups: the basement and the cover (Fig. 2) (Akartuna, 1962; Boray *et al.* 1973; Konuk, 1977; Yağmurlu, 1980; Başarır & Konuk, 1981; Erdoğan, 1990; Bozkurt *et al.* 1993; Genç *et al.* 2001; Uzel & Sözbilir, 2008).

The basement rocks comprise two different geological features: the Menderes Massif that crops out in the eastern part and the Bornova flysch that
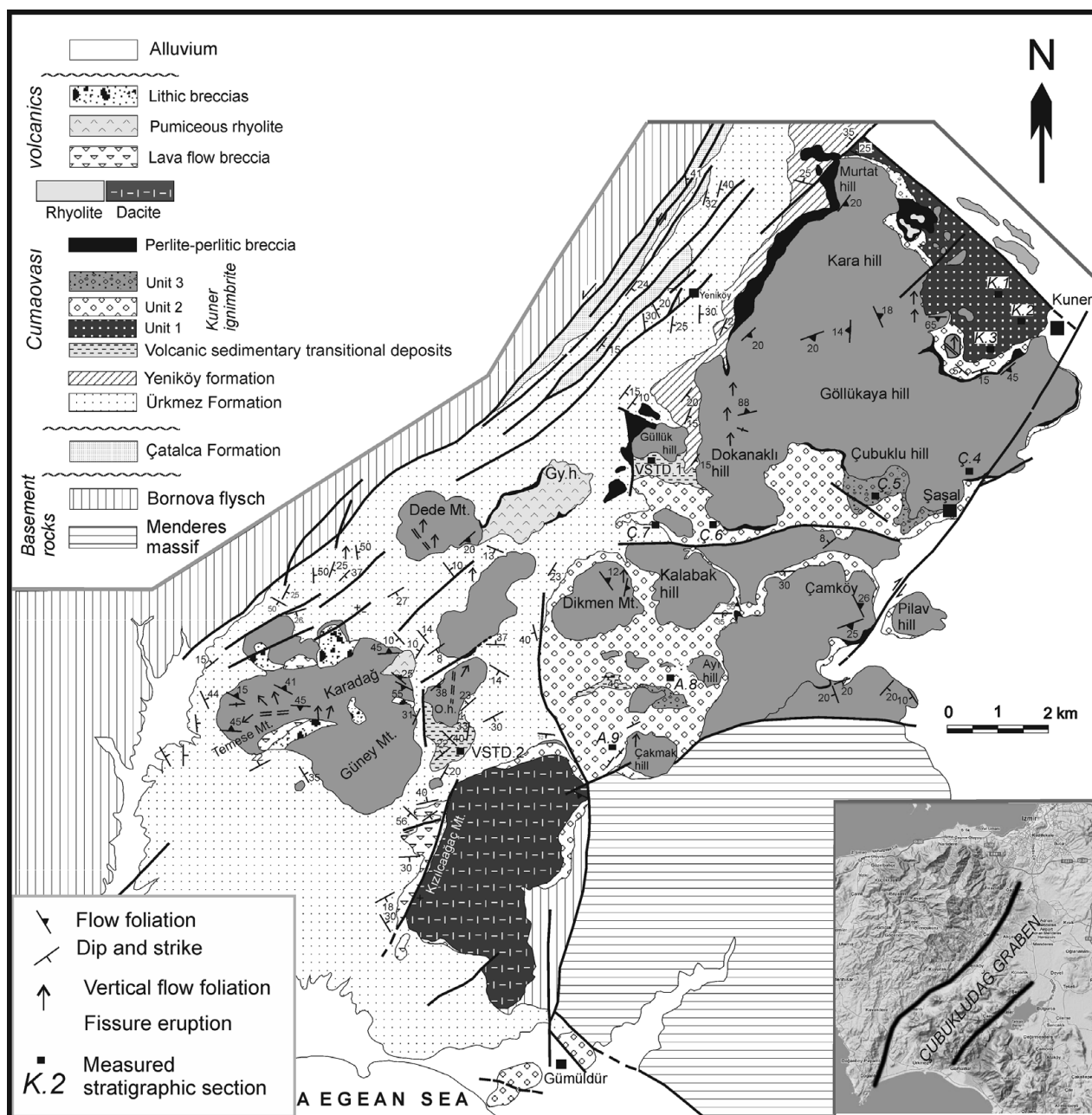
Figure 2. Geological map of the Çubukludağ Graben and surrounding region (modified after Genç *et al*. 2001). Gy.h. – Gülyaka Hill; O.h. – Orta Hill. Base map of the inset is from http://www.maps.google.com. See the online Supplementary Material at http://journals.cambridge.org/geo for a full colour version of this figure.

crops out in the western shoulders of the basin, representing the horst areas. The graben infill is also composed of two different sedimentary rock deposits: the Çatalca and the Ürkmez formations at the bottom and the Yeniköy Formation together with the Cumaovası volcanic rocks that form the upper part of the succession (Genç *et al*. 2001). The Çatalca Formation is a lacustrine flysch-like succession which is Lower Miocene in age. The overlying Ürkmez Formation is represented by continental red-beds. The Yeniköy Formation, Upper Miocene – Pliocene in age (Akartuna, 1962), contains freshwater gastropoda and lamellibranchia-rich fauna, and was deposited in a low-energy lacustrine environment (Akartuna, 1962). These formations alternate with the pyroclastic deposits of the

Cumaovası volcanic rocks, which were deposited sub-aerially around the northern part of the study area.

Cumaovası volcanic units are the youngest and most dominant rock group within the graben infill. The volcanic rocks cover an area of *c.* 350 km^2 and are represented mostly by silicic lava domes and fissure-erupted lava. The K–Ar ages of the unit obtained from this study are 17.2±0.5 and 17.9±0.6 Ma corresponding to the late Early Miocene (Karacık *et al.* 2013). This age span contradicts previous K–Ar (12.5 Ma; Borsi *et al.* 1972) and stratigraphic ages which were based on the fossil ages of the Yeniköy Formation; we suggest this needs further critical revision.

Figure 2 shows the regional distribution of silicic lavas and related pyroclastic deposits.

Digital-map-based calculations indicate that the total areal distribution of the lavas and pyroclastics are 55 km^2 and 70 km^2, respectively. The volume of the pyroclastic deposits is 3 km^3 and of the lava flows is 11 km^3 (Dacites: 0.877 km^3, rhyolites: 10.23 km^3), totalling 14 km^3. We used average thicknesses for the units; in this way, minimum volume is calculated.

The Cumaovası volcanic rocks are relatively young members of the Neogene volcanic rocks of Western Anatolia. The silicic volcanism of the Çubukludağ Graben is particularly interesting in view of the unusual conditions of their origin and the fair preservation of eruption centres and their products. The volcanic activity is composed of two main stages: (1) the pyroclastic-dominated explosive stage formed from pyroclastic density currents; and (2) the lava-dominated stage, characterized by widespread silicic (rhyolite-dacite) domes and fissure eruptions and related flow breccias. The early stage of pyroclastic activity was characterized by highly explosive phreatomagmatic (hydrovolcanic) base-surge-forming eruptions that produced ring-like tuff deposits. This was followed by the collapse of the eruption column, producing the pyroclastic density currents (PDCs). The main stage of volcanism occured as lava extrusions, seen as domes along minor fractures as well as major regional tectonic features. Hot springs and fumerolic activity identify the last stage of volcanism in the Cumaovası Graben.

The areal distribution and eruption of the Cumaovası volcanic rocks are mainly controlled by the two graben-related fault systems: the SW–NE-trending oblique faults with their antithetic components (Genç *et al.* 2001; Uzel & Sözbilir, 2008) and the approximate E–W-trending normal faults. SW–NE-trending oblique faults deformed the Early–Middle Miocene Çatalca Formation and controlled the deposition of the Ürkmez Formation. Some coeval faults display opposite slip sense to the master faults and are perpendicular (or nearly perpendicular) to them. Such faults are identified as anti-riedels by Uzel & Sözbilir (2008). Some good examples can be found in the graben between Güney Mt and Güllük Hill, although most of the rhyolitic domes display a trend parallel to the master faults and the small domes at the SW parts of this area, and in the dome succession between Kara Mt and Dede Mt. At Kızılağaç Mt, dacitic lavas poured along the fault zone at the western side of the mountain. As shown in Figure 2, there are a number of minor faults between the western and eastern master faults of the Çubukludağ Graben. Some of them acted as the opening cracks or trans-extensional faults along which dacitic and rhyolitic lavas rose to the surface, for example the Dikmen and Kalabak domes which lie along the nearly E–W-trending normal fault or the Temese rhyolite dome (Fig. 2) which was formed along a cryptic and E–W-trending opening crack.

Some faults which were formed under the same tectonic phase as the master faults above cut and displace some of the domes, suggesting that such faults

were rejuvenated after the formation of the rhyolitic domes. The western-boundary fault of the Çubukludağ Graben (i.e. Orhanlı fault zone, Genç *et al.* 2001) is an active fault producing earthquakes (e.g. Doğanbey earthquake, Ms 5.9, 6 October 1992; Türkelli *et al.* 1995). The fault-plane solution which belongs to this earthquake indicates that the Orhanlı fault operates as a right-lateral strike-slip fault (Türkelli *et al.* 1990, 1995; Ocakoğlu *et al.* 2004; Ö. Emre *et al.*, unpubl. report, 2005). The hot springs in the Tuzla and Cumalı regions along this fault zone are indications of its recent activity (Eşder & Şimşek, 1975; Tarcan & Gemici, 2003; Drahor & Berge, 2006). Genç *et al.* (2001) discovered that the Orhanlı fault zone originally operated as a sinistral strike-slip fault. According to Uzel & Sözbilir (2008) the fault zone initially operated as sinistral and then changed to dextral strike-slip motion.

In the central part of the study area the Cumaovası volcanic rocks are intercalated with the topmost levels of the Ürkmez Formation, indicating the temporal association with the volcanic and sedimentary rocks, which are the fault-controlled deposits. This close relationship between the volcanic and sedimentary rocks and the areal distribution of the domes and faults reveals that the Cumaovası volcanic rocks probably rose through and erupted along the faults, thus controlling the sedimentation in the Çubukludağ Graben basin.

3. Facies description of pyroclastic units

Two different volcano-stratigraphic levels are identified in the pyroclastic succession of the Cumaovası volcanic rocks. The lowermost group is volcanic-sedimentary transitional deposits (VSTD) which crop out around the Orta and Güllük hills in the central part of the graben (Fig. 2). Widespread pyroclastic units of this group level are tuffs and pumice-rich lapilli tuffs, intercalated with sedimentary deposits. Above this, the second main layer is the Kuner ignimbrite which is composed of pumiceous ash tuffs, pumice lapilli tuffs and breccia deposits (Figs 2, 3, 4). The features of these units are documented in detail in the following sections. We have followed a non-genetic terminology, based upon internal sedimentary structure and grain size in order to define the lithofacies. We based our facies definitions on the classifications of Sohn & Chough (1989) and Branney & Kokelaar (2002).

3.a. Volcanic-sedimentary transitional deposits (VSTDs)

3.a.1. Description

The initial products of the explosive stage are mainly represented by pyroclastic-dominated sedimentary deposits. At the bottom of the sequence, finely laminated ash tuffs alternate with the lacustrine sedimentary rocks of the Yeniköy Formation. Stratigraphic sections from
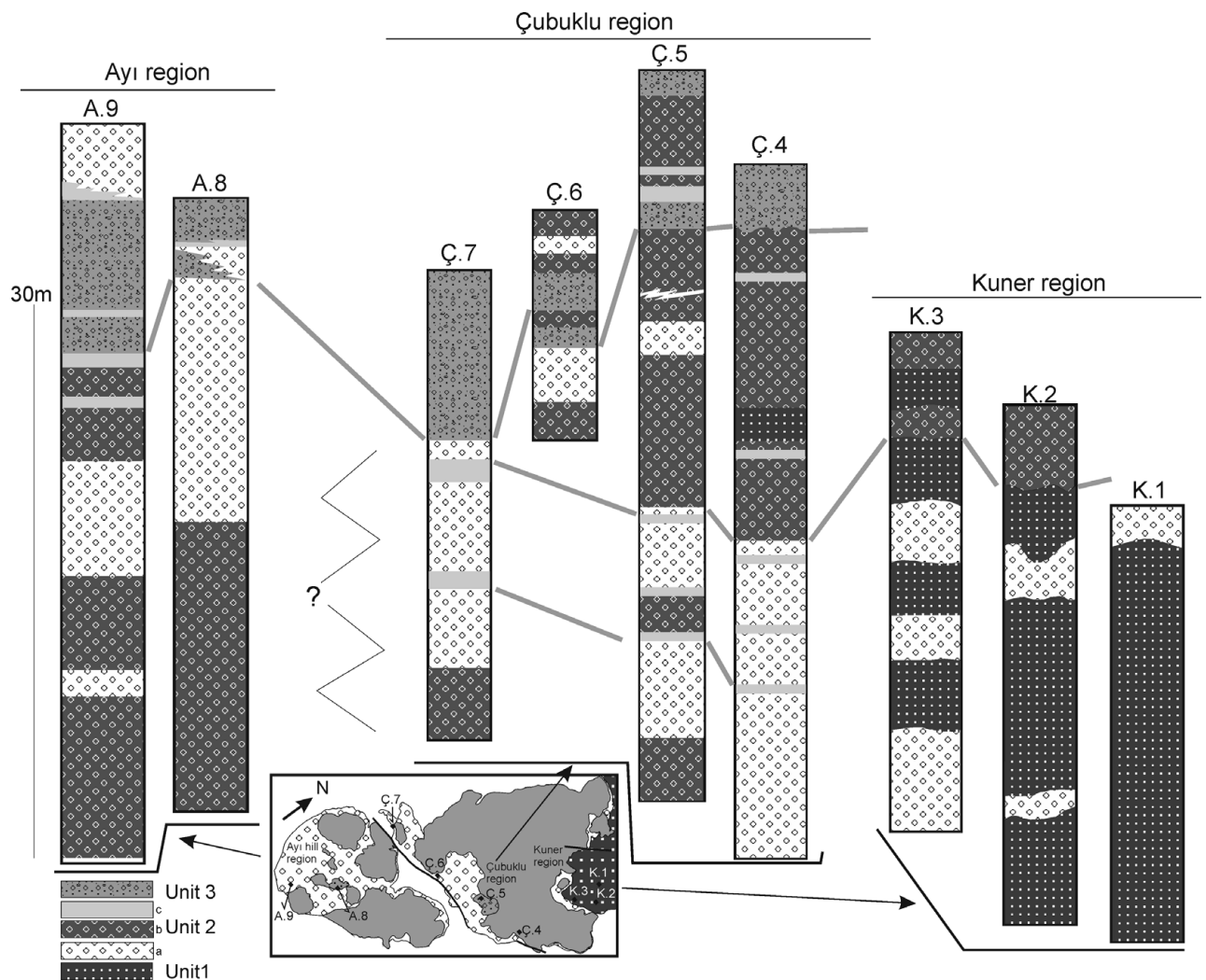
Figure 3. Correlation diagram of general stratigraphic sections from the Kuner ignimbrite. For section locations, see Figure 2. See the online Supplementary Material at http://journals.cambridge.org/geo for a full colour version of this figure.
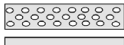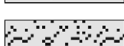
the Orta Hill region and the southern part of the Güllük Hill (VSTD.1 and VSTD.2 in Figs 2, 5) clearly show the details of this deposition. The common lithologies of the transitional zone are fine- to medium-grained volcaniclastic siltstone, sandstone and marl alternating with pumice-rich volcanic deposits. The deposits are thinly bedded and cross-laminated (wavelength 1 m; height 30 cm) in some places. The sizes of pumices are 0.3–1 cm (maximum 2–3 cm) and rarely seen lithic fragments are 0.3 cm (maximum 1 cm). Local concentrations of coarse grains form lensoidal or irregular patches with gradational contacts. These deposits pass gradually upwards into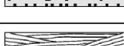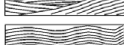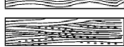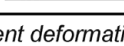 thinly bedded tuff – lapilli tuff (bLT – bT), diffuse-stratified lapilli tuff, diffuse-stratified tuff (dsLT, dsT) and pumice-rich tuff (pT). The main components of these deposits are angular to subrounded pumices (0.5–3 cm) and rare lithic fragments, which are larger than those found lower down (3–10 cm in average, maximum 20 cm in diameter) and were derived mainly from the metamorphic basement rocks. Some of the siltstone and shale fragments are up to an average of 40–60 cm. In some places the lithic-rich tuffs pass upwards to vesiculated pumice tuff with rare, rounded lithic fragments.

3.a.2. Interpretation

The areal distribution, depositional characteristics and lithological and sedimentological features of this sedimentary deposit indicate air-fall material laid down in a lacustrine environment and then reworked in shallow water. Fine lamination, cross-bedding and lensoidal pebble-rich layers are indicators of a low-energy shallow-water environment. The existence of these deposits at the transition zone between the red-beds of the Ürkmez Formation and the pyroclastic units therefore suggest that, during the deposition of the continental red-beds, water on palaeotopography was present.

3.b. Pyroclastic deposits: Kuner ignimbrite

The Kuner ignimbrite possesses almost every kind of pyroclastic deposit found in the Çubukludağ Graben but mainly consists of pumiceous lapilli tuff and tuff (ash) (Figs 2, 3, 4). All the lithofacies are dacitic/rhyolitic in composition and lithified. The thickest (100–150 m) and the coarsest deposits are located in the central part of the Çubukludağ

	Lithofacies code		Description	Interpretation	Section/Outcrop
U3	mlBr		massive lithic breccia	Coarse lithic breccia rich proximal facieses of the PDCs	Şaşal village, Çubuklu, Ayı hills; sections Ç4-5-7,A8-9
U2	U2c	mTpel-mTcpel/ sTpel-sTcpel	massive and/or stratified ash tuff with ash and coated pellets	Pyroclastic density currents related fall deposits and/or co ignimbrite ash pellet fallout deposits	Şaşal village and north of Kalabak hill; sections Ç4-7
		bLT-bT	thin-bedded, lapilli tuff-tuff		
	U2b	fpoorT	fines poor tuff (fpoorT)	Rapid progressive aggradation from granular fluid- based PDCs	Şaşal village, Çubuklu, Dokanaklı, Kalabak, Çakmak, Ayı hills; sections K2-3,Ç4-7,A8-9
		mLT-mT	massive lapilli tuff-tuff with lithic fragments	Deposited from ash-rich parts of PDCs by rapid progressive aggradation from a high-concentration fluid escape-dominated depositional flow-boundary	
	U2a	dsT-dsLT	diffuse-stratified lapilli-tuff rare lithic fragments -vessiculated tuff		
U1	U1b	xsT-xsLT	cross-stratified tuff-lapilli tuff	Chancing of depositional style from phretomagmatic fallout to flow deposits (PDCs); tractional sedimentation from fully dilute PDC	Kuner region; sections K1-K2-K3, Çubuklu region; Ç4
	U1a	//sT-sLT	parallel-stratified tuff-lapilli tuff	Main phretomagmatic phase; phretomagmatic eruptions derived fall out deposits	
		//bpLT-//bT	parallel-bedded pumice lapilli tuff-tuff		

soft sd: soft sediment deformation
cw: carbonized wood fragments
ad: antidune

l: lithic
ves: vesiculated
lenslBr: lens of lithic-rich breccia
lenspL: lens of lapilli-rich deposits
ub: undulatory bedded

Tube pumice
Carbonized wood
acc: Accretional lapilli

Figure 4. Descriptions and interpretations of the units from Kuner ignimbrite, with all the abbreviations and the symbols for the Kuner ignimbrite. See the online Supplementary Material at http://journals.cambridge.org/geo for a full colour version of this figure.

Graben. Nine stratigraphic sections through the Kuner ignimbrite have been measured in order to establish their stratigraphic sequence and depositional nature (Fig. 3), demonstrating that it is composed of three laterally continuous lithostratigraphic sections (Fig. 4) described in the following sections.

3.b.1. Unit 1

3.b.1.a. Description

These deposits mainly crop out around the Kuner village in the NE part of the Çubukludağ Graben, the exposed area being *c.* 2 × 3 km in size. They are very fine grained, typically with fine ash to lapilli-sized pumice-rich deposits, displaying well-developed millimetre- to centimetre-scale stratification (see the measured stratigraphic sections K.1, K.2 and K.3 in Fig. 6). Each shows a variety of lithofacies based on variations in grain size, composition and depositional structures. Unit 1 mostly comprises well-sorted parallel- and cross-stratified ash tuff, lapilli tuff (//bpL, //sT, xsT and bLT) and pumice lapilli tuff (Fig. 6). This subunit of alternate composition has a total thickness range of 10–25 m. Although components within unit 1 are very similar, they can easily be differentiated into 2 subgroups on the basis of the sedimentary structures.

Subunit 1a shows an alternate layering of white to grey, thin- and parallel-bedded fine-pumice lapilli (//bpL) and parallel stratified ash tuff layers (//sT) that mainly crop out in the Kuner pumice quarry (Fig. 6). With a thickness of *c.* 5–15 m and a very homogeneous lithology, these stratified deposits consist of juvenile clasts of fine pumice (1–1.5 cm), medium to coarse ash and small amounts of quartz and feldspar crystals. There is a normal grading of pumices in the upper part. A distinctive feature here is horizontal (planar) bedding with alternate layers of different-sized ash- and lapilli-rich layers. Each layer is laterally continuous across exposures and has uniform thickness (Fig. 7a). The bedding, however, is of varying thickness; pyroclast size varies between 5 and 20 cm. Alternation intervals are very narrow (5–10 cm) between fine ash and lapilli (bLT) in the upper parts of the pumice quarry. Lithic fragments are very few and 0.5–1 cm in diameter. Coarse rhyolite and perlite fragments, white- to grey-coloured and subrounded to angular in shape are occasionally seen. They have fairly long-wavelength (1–2 m) undulatory bedding structures and also sinusoidal ripple-drift laminations of short wavelength (0.5–1 m) in the middle layers of the K.1 section (Fig. 7b). Well-developed undulatory-layered structures, rills and gullies of various scales are common in the pumice quarry. This structure is similar to either soft sediment deformation structures (settlement structure, i.e. load cast) and/or syn-erosional structures (rills and gullies) (Fig. 7c, d). The width and depth ranges of the small rills are a few centimetres. Some synsedimentary faults are also common (Fig. 7a, c). The V- and U-shaped cross-sectional profiles vary over 40–50 cm in depth and 2–5 m in width and occur along the same stratigraphic horizons.

Subunit 1b is the lateral continuity and upper layers of subunit 1a. It is composed of similar lithologies such as fine-grained cross-stratified pumiceous ash tuff – lapilli tuff (xsT–xsLT) and parallel-bedded pumice lapilli tuff (//bpLT) (Fig. 8a); the main difference between the subunits is the very-well-developed cross-stratification and undulatory bedding. Although they are variable in most places, the wavelengths of cross beddings are 60–80 cm and the amplitude is generally 30–40 cm (Fig. 8b). They form multiple thin-lensoidal cross-sets and pass into undulatory bedded deposits (Fig. 8c). In places the wavelengths are larger and vary over the range 0.5–7 m where amplitudes are 0.2–2 m in the lapilli tuffs and tuffs (Fig. 8c, d).

VSTD.1
South of Orta Hill

Thickness

- 3m — P: 3-10 cm, LF: 20 cm max. 60 cm
- 1m — P: 1-3cm
- 2m — LF:10-15 cm max 20 cm
- 20cm — Ash tuff
- 2-2.5m — LF:3-5cm, P:1-2 cm
- LF:3-4 cm, max. 20-30 cm
- 8m
- Rare LF: 0.2-0.5 cm max. 3 cm
- 30 cm
- 40 cm
- 35cm
- 90cm
- 30cm
- 10cm — Siltstone-mudstone
- 10m
- LF:5-10cm
- LF:40-60 cm P:0.5, max 1cm
- 2m — LF: 3-7 cm max.15 cm P: 0.2-3 cm
- 3m
- 70cm — P: 0.3-1cm, max. 2-3cm; LF: 0.3, max. 1cm
- 4.5m — LF:3-10cm max.15 cm P:0.2-3cm
- 2m — Pumice rich
- 30-50 cm thick pebble pods or channels Pebble: 0.5-2cm rarely 10-5cm
- 5m — Angular pumice rich (2-3 cm) zone
- 30cm
- 2m — P: 0.5, max.1cm LF: 0.5-1cm
- 20cm — P:angular-sub angular 2-4cm
- 1.2m — Red coloured, reverse graded LF:0.2-0.3 cm in the bottom
- 40cm — 3 cm in the top, P: 1 cm
- 2m — LF: 0.5-1cm
- 35-40cm
- 40cm
- 50cm
- 80cm — Marl with fine pebble and pumice
- 60cm — Red-pink colour with 3cm mud nodules
- 1m — P:1-3 cm, LF:1cm
- 60cm
- 10cm — Pink-red colour, limestone-chert pebble (1-3cm) rich zone
- 70cm

VSTD.2
South of Güllük Hill

Thickness

- 2m
- 50cm — Fine laminated siltstone-claystone with 35-45 cm thick pumice rich zone (1 cm, angular)
- 2-3m — Angular tuff fragments (20 cm)
- 2m — Well sorted and graded
- 40cm — Reverse graded (0.2 cm-1 cm)
- 2m — 2-2.5 max15-20 cm size siltstone lenses Ash tuff coarse sandstone alternation
- Coarse grained sandstone
- Fine sandstone, rare pebble
- 75cm — Fine laminated tuff, rarely mudstone blocks (8-10 cm)
- 1.5m — Pumice rich volcaniclastic fine pebble-sandstone
- 50cm — LF:10-5cm, P:3-5cm
- 1m — LF:0.2-0.5 cm max. 1cm
- 10-15cm
- 2m — Well sorted, normal graded P:0.2-1.5 cm
- 40cm
- 1m

KEY

- Fines poor tuff
- Massive lapilli tuff
- Massive lithic breccia
- Thin-bedded, lapilli-tuff/ash
- Marl
- Volcaniclastic siltstone-sandstone
- Pumice rich zone
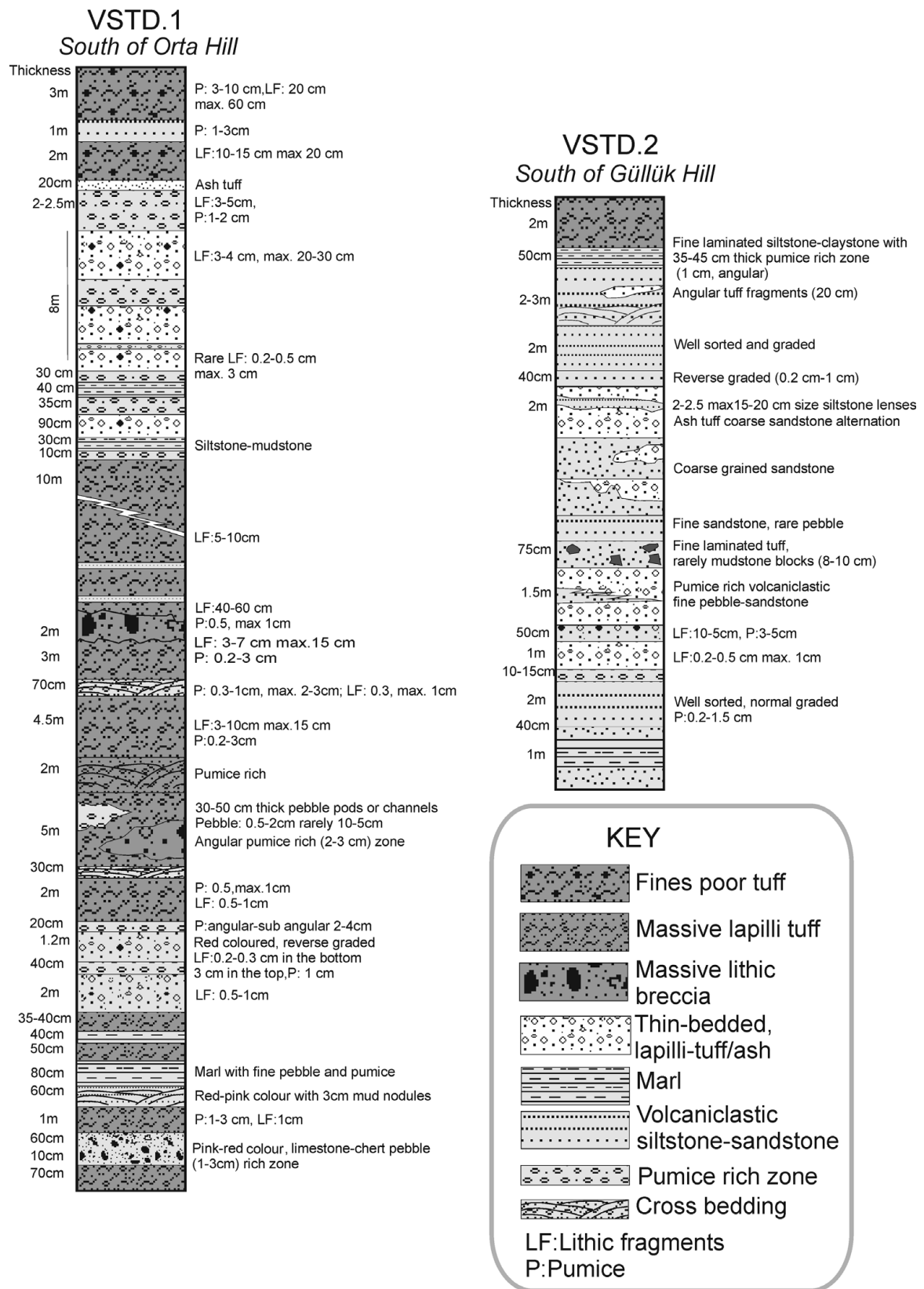- Cross bedding

LF:Lithic fragments
P:Pumice

Figure 5. Measured stratigraphic sections of the volcanic sedimentary transitional deposits from south of Orta Hill region (VSTD.1) and southern part of the Güllük Hill (VSTD.2). See the online Supplementary Material at http://journals.cambridge.org/geo for a full colour version of this figure.

The thin-bedded pumice lapilli tuffs display locally normal grading. Bedding is laterally persistent (in 20–30 m scale) with sharp boundaries between the beds. Different-sized slumping structures in the pumice lapilli tuff (Fig. 8e) and rare block-impact structures are seen in the Kuner 1 section (Fig. 8f). Lens-type, lapilli-rich deposits (lenspL) show lenticular geometry and alternate with the stratified tuff layers (section K.2).
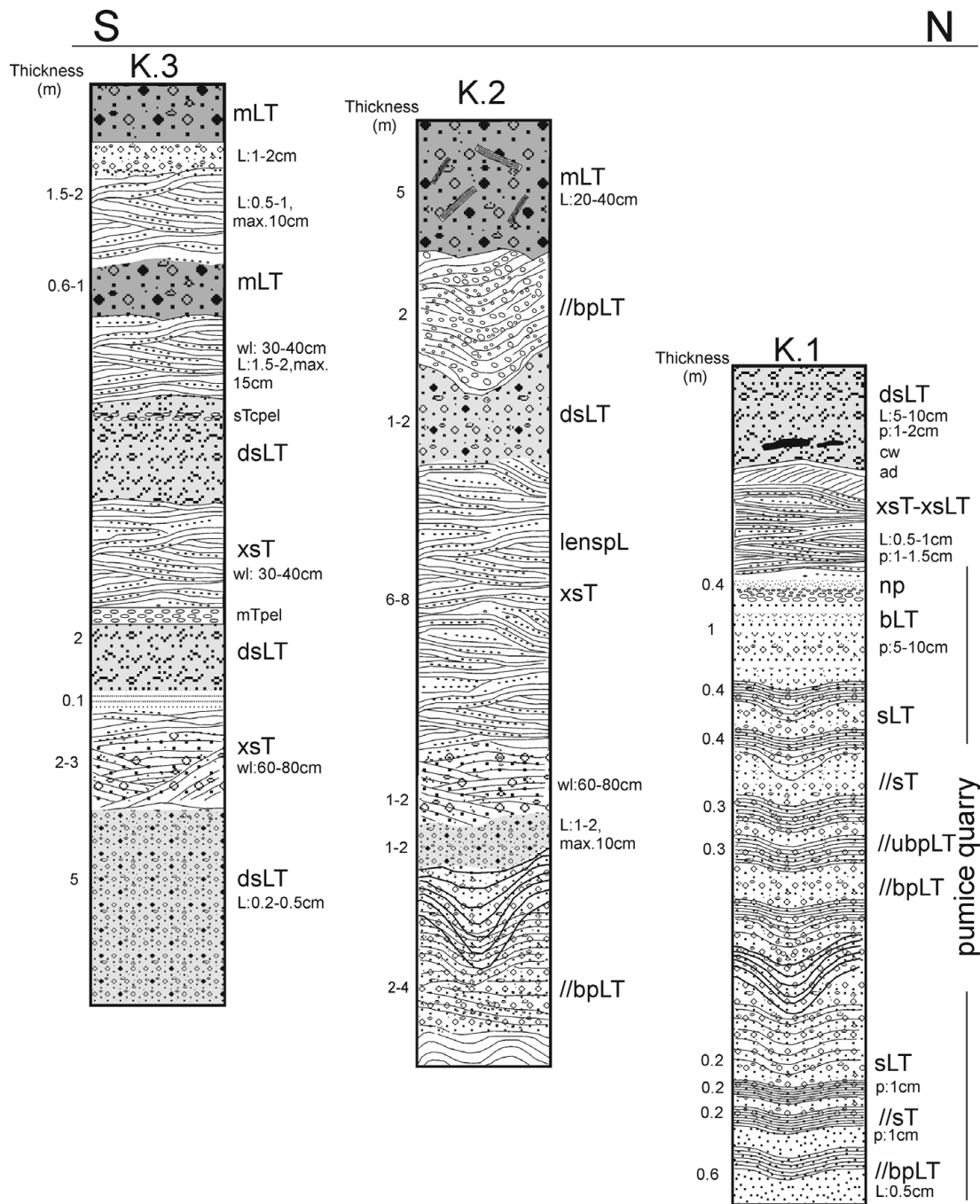
Figure 6. Measured stratigraphic sections from Kuner village and surrounding region. Figure 4 lists all abbreviations and legends for the units. See the online Supplementary Material at http://journals.cambridge.org/geo for a full colour version of this figure.

These lensoidal deposits reach up to 2 m in width at some places. Fine-grained ash-pumice tuff deposits show close folding near Kuner village (Fig. 8g). The wavelength of the folds varies over the range 2–4 m (Fig. 8g, h). The trend of the fold axis is N–S and the folded zone passes through into undulatory and/or cross-bedded layers of greater wavelength, reaching 10 m in some localities. The correlation of discrete horizons between outcrops is exceptionally difficult because of the discontinuity and position of the outcrops.

This unit can also be seen as thin interactions with lateral discontinuities in the Çubukludağ region which

are composed of pumice lapilli tuff and fine pumiceous ash tuff alternations with rare lithic fragments (10 cm) (Fig. 9; Ç.4). Their thickness varies over the range 2–3 m. The average wavelength of cross-bedding is 70 cm at the bottom and 20–30 cm in the upper layers.

3.b.1.b. Interpretation

As stated, all components in unit 1 are very fine grained, derived mainly (90%) from juvenile materials. Subunit 1a is commonly planar and persists over a long distance. The existence of syndepositional deformation is partly related to small-scale normal and reverse faults. Shock waves caused by powerful synchronous
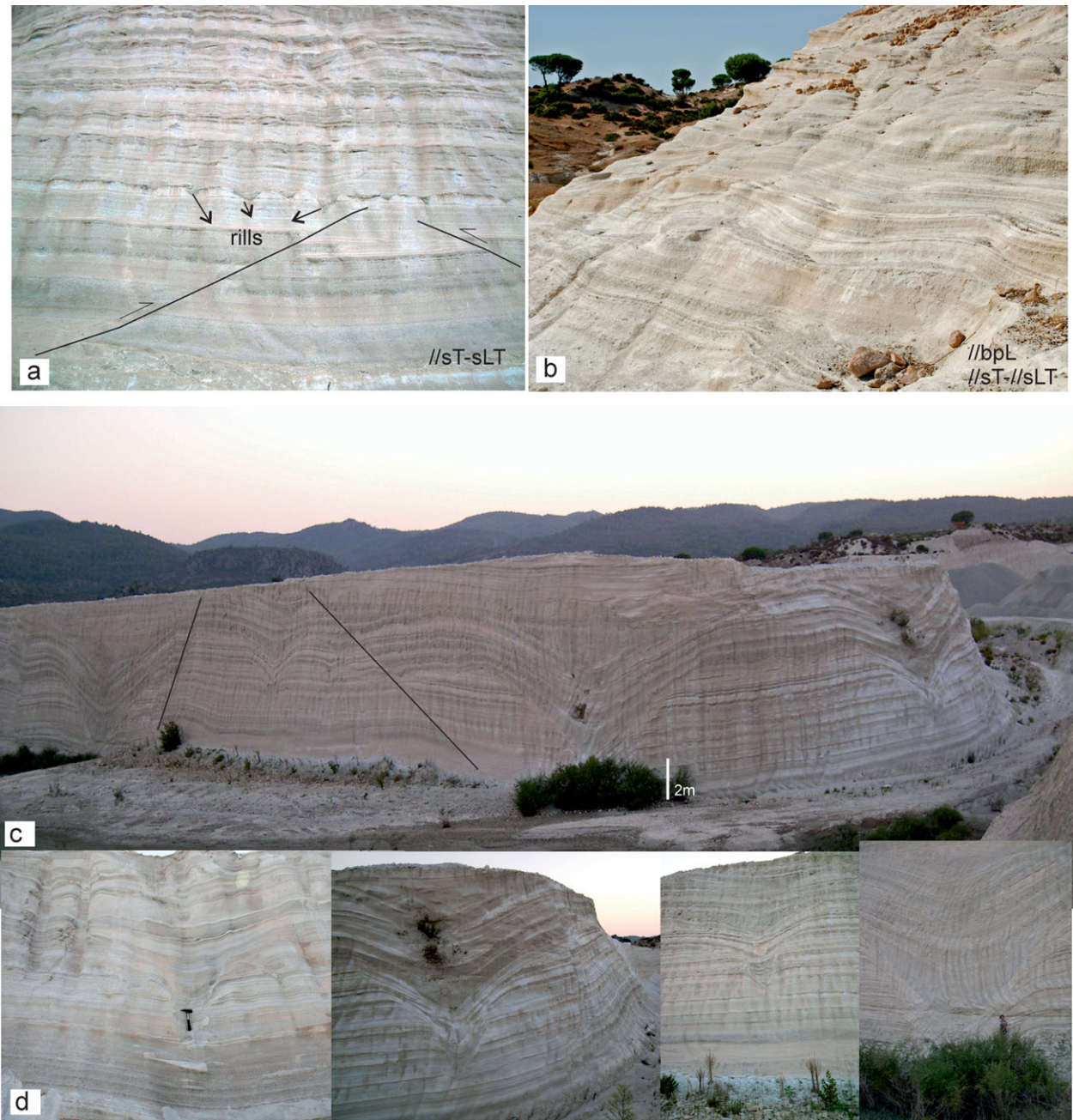
Figure 7. (Colour online) (a) General view of unit 1 parallel-bedded pumice tuff and lapilli tuff alternation with erosion channels (rills). The unit is cut by several small faults. (b) General view of sinusoidal ripple-drift laminations of short wavelength on the parallel-stratified tuff-pumice tuff of unit 1. (c) Different-sized settlement structures, erosion channels (gullies) and/or soft sediment deformation structures with the syndepositional faults (marked by thin black lines). (d) Detailed views of the different-sized gullies and/or erosional channels. Gullies display multiple episodes of cut-and-fill structures which are preserved by parallel bedding.

(or accompanying) eruptions may have caused the load structures and soft sediment deformations. The different-sized erosion channels (rills and gullies), very common in the middle part of the unit and seen in the volcanic successions of Koko Crater in Hawaii, developed as a result of the overland flow of subsurface water (Bluth, 2004). Erosion channels were possibly produced by surface water from syn-eruptive condensed steam in the pyroclastic currents. In addition to this, perfect sorting, parallel thin bedding and lateral continuity of internal grading pattern suggest phreatomagmatic fallout deposition in subunit 1a.

Within subunit 1b deposits are mostly composed of fine clasts derived from fluid turbulence. The most significant feature of these is the existence of sand-wave structures. Pinch and swell structures produce laterally lensoidal beds in fine-grained pyroclastic deposits. Although the ash and lapilli-sized tuff units are mostly parallel stratified, they contain undulations with wide amplitude and a very regular form. The waves are gently sloped and generally have long wavelength and low amplitude, often grading laterally into planar beds and ultimately passing into faint laminations. Several metres to centimetre-scale cross-stratification passes
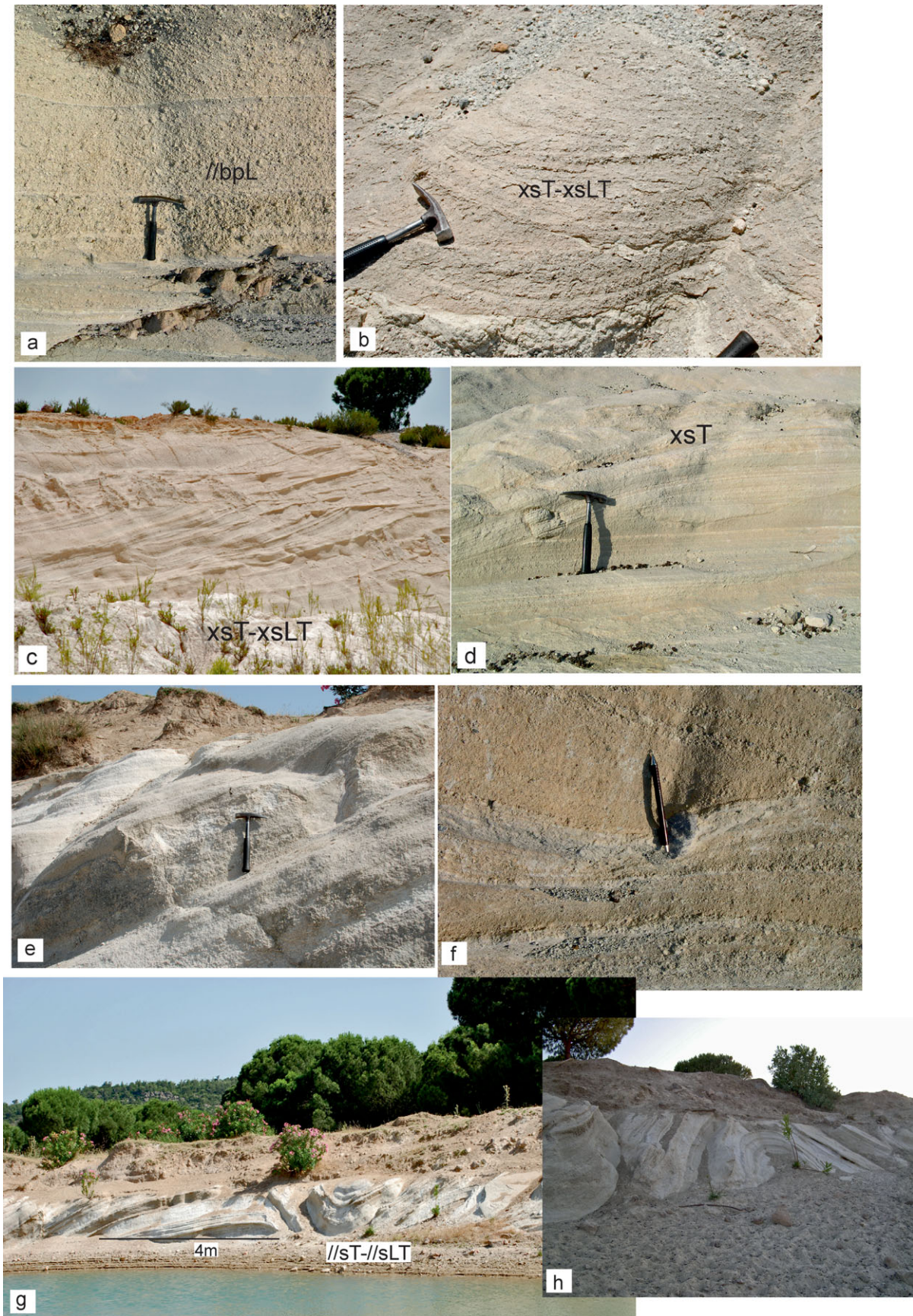
Figure 8. (Colour online) (a) Detailed view from the parallel-stratified pumice lapilli tuff. (b) Cross-stratified tuff-lapilli tuff. Festooned dunes direction of transport is perpendicular to the plane of the paper. (c) Dune structures of the pumice tuff-pumice lapilli tuff; wavelength 2–3 m. (d) Close-up of dune structure in the cross-stratified tuff. Head of hammer indicates blowing side of the deposits. (e) Slump structures in the parallel-bedded lapilli tuff. Undulated layer between the parallel-bedded lapilli tuff is located at the head of the hammer. (f) Example of the impact structures. Ballistic block (6 cm) in the pumice-lapilli tuff deposits. (g) Close folded pumice lapilli tuff deposits. (h) Close-up of (g).
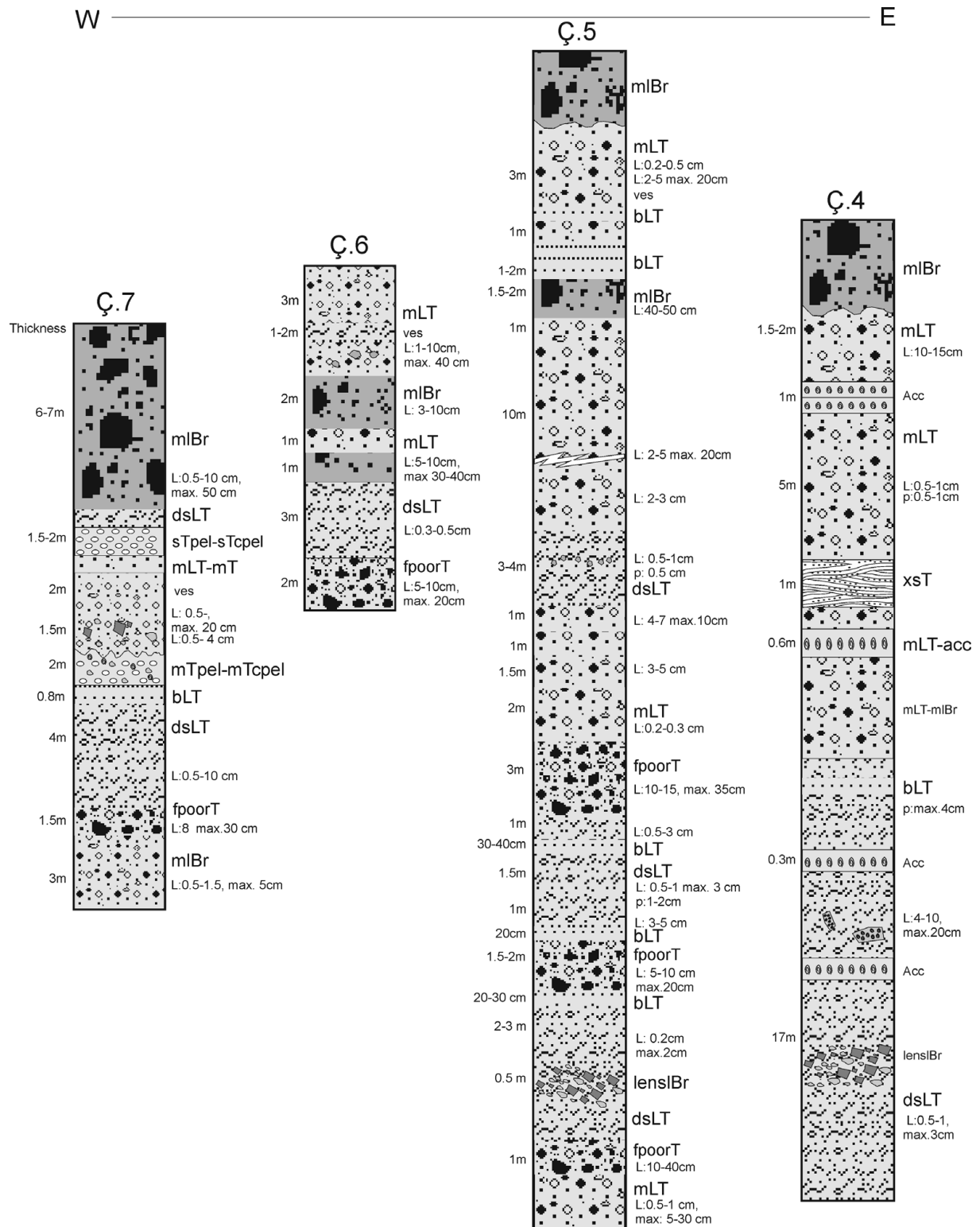
Figure 9. Measured stratigraphic sections from the southern part of the Çubuklu–Dokanaklı hills and Şaşal village region. See Figure 4 for abbreviations and legends for the units. See the online Supplementary Material at http://journals.cambridge.org/geo for a full colour version of this figure.

laterally to thin lenticular cross-sets (sand-waves) and undulatory bedded tuffs. The existence of asymmetric block-impact structures may be explained by the effect of ballistic ejecta in the Kuner ignimbrite. The vertical and lateral changes of the massive and cross-stratified layers further imply that the currents underwent rapid temporal changes, for example in particle concentration

and velocity. This is seen in the Glaramara tuff in Scafell caldera (Brown *et al.* 2007).

Although the cross-stratifications indicate a highly unsteady environment, the presence of thin lenticular cross-sets is a clue to the very low aggregation rate. These types of deposits are similar to the 'starved' dunes where unsteady currents constructed

well-developed sand-waves (Fig. 8c) (e.g. Branney & Kokelaar, 2002). On the other hand, the presence of meso-scale folding and close-folding with different amplitudes demonstrates their more energetic origin. Similar structures were identified as radial channels in the Ramadas volcanic centre in Argentina by Tait *et al.* (2009). Radial channels are related to the propagation of pyroclastic surge currents, which are filled by lapilli and ash beds. Pumice-rich deposits indicate that the pumices were segregated during the transport of the deposits by PDCs.

Structural features such as parallel, cross-stratification and good sorting are indicators of deposition from traction-dominated fully dilute PDCs (e.g. Branney & Kokelaar, 2002). Subunit 1b deposits are therefore interpreted as an ignimbrite derived from the non-uniform ash- and pumice-rich low-concentration PDCs. All features outlined above reveal clearly that unit 1, as a whole, derived from the phreatomagmatic eruption(s) both as fall deposits from eruption plumes and accompanied ash-rich pyroclastic density currents.

3.b.2. Unit 2

3.b.2.a. Description

Unit 2 is the most widespread and the thickest of the volcanic succession. Although appearing in thin layers within the Kuner region, it becomes thicker and very commonplace in the central (Çubukludağ region) and SW parts (Ayı region) of the graben (Figs 2, 3, 9).

The main lithology of this unit can be divided into three subgroups: (1) an alternation of diffuse-stratified tuff – lapilli tuff (dsT–dsLT) (subunit 2a); (2) massive lapilli tuff – tuff with lithic fragments (mLT–mT) and fines-poor tuff (fpoorT) (subunit 2b); and (3) subunit 2c formed from thin-bedded lapilli tuff – tuff (bLT–bT) and ash tuff with ash pellets and accretionary lapilli (mTpel–mTcpel–sTcpel). The area as a whole is rich in white-coloured lapilli-sized sub-angular to rounded pumices and crystal fragments (quartz, biotite and sanidine) and contains abundant different-sized rhyolite, obsidian and perlite fragments. A white-coloured matrix is also composed of fine ash and small pumice fragments. Sub-angular pumice groups were flattened in some layers, but welding is not recognized in any parts of the sequence. Zeolitic alteration is common, especially in pumiceous ash tuffs. Lithological features change in only a short distance along their lateral and horizontal extent and shown as measured stratigraphic sections (Fig. 9).

Subunit 2a is mainly located at the bottom of the volcanic succession in the Çubukludağ region (sections Ç.4–7), but in the upper and middle layers in the Ayı region (sections A.8 and A.9) (Figs 9, 10). It consists of diffuse-stratified tuff and lapilli-tuff (dsT–dsLT) formed from lapilli- and ash-sized pumice fragments in a fine ash matrix (Fig. 11a). They display well-developed millimetre- to centimetre-scale layering. Diffuse stratification, mainly subparallel and continuous over a large area, may pass into the sections

that exhibit low-angle truncations and cross-stratified subunits in some places (Fig. 11b). The deposits here are generally poorly sorted with crudely bedded pumice-rich deposits and few lithic fragments. Pumices are 0.5–2 cm, rarely reaching 4 cm in diameter. The lithic fragments are mainly angular to sub-angular rhyolite, perlite and rare metamorphic rock fragments. Average lithic sizes are 0.5–1 cm but range over 0.2–0.5 cm (maximum 5–10 cm) in the Kuner region and 0.2–1 cm (maximum 3 – (rarely) 10 cm) in Çubukludağ region. Rarely are very large blocks (50–60 cm and a few of maximum 1.5 m) seen around the Ayı region (Fig. 11e). There are thick (0.5–1.5 m) angular lithic-fragment-rich layers that are classified as lens LBr in the Şaşal, Çubuklu and Kalabak sections (Figs 9, 10). In these layers, the maximum lithic fragment size is 20 cm in diameter. Carbonized wood fragments can be found here and they lie parallel to stratification of the lapilli tuff (Fig. 11c). The upper layer is represented by vesiculated tuff in some places (sections; Ç.5–7 and Fig. 11d). The different-sized (0. 3–1 cm) vesicles are elongated along the flow direction in some layers and are similar to those vesicular tuffs described by Lorenz (1974). In the northern part of the Kalabak Hill, there are well-sorted, rare lithic and crystal fragment-bearing pumiceous ash tuffs. The Çubuklu Hill section is however the thickest (*c.* 50 m), ordered in a continuous sequence of alternate pumice-rich dsLT and mLT deposits (Fig. 11f).

Subunit 2b mostly crops out within the upper levels of the Çubukludağ region but at the base of the Ayı area (sections A.8 and A.9 in Fig. 10). Although many features are the same as subunit 2a, the texture and size of the lithic fragments differ. Here we see lithic-fragment-rich massive lapilli tuff and pumiceous ash tuff (mLT) beside the massive tuff (mT) lithic-fragment-rich layers. This is interspersed with alternate layers of fines-poor tuff (fpoorT). These units alternate laterally and vertically with the upper part of unit 2 in specific places (K.3 section in Fig. 6) and are also covered by an unconformity in the K.2 section, illustrated in Figure 6 (Fig. 12a). The main components are pumices, ash, crystal fragments and rare lithic fragments in an ash and very fine ash matrix. There is no internal stratification and the massive texture is the distinctive feature of this subunit (Fig. 12a, b).

The pumice deposit is poorly to very-poorly sorted with pumice clasts that are 0.5–1 cm in general and lithic fragments that are 0.5–1 cm on average with a maximum diameter of up to 5–10 cm (Fig. 12a). We have identified singular large (30 cm) semi-rounded to angular lithic fragment-rich layers (Fig. 12c) and lithic breccia lobes (Fig. 12d). The fines-poor tuff (fpoorT) is coarse grained, lithic-fragment rich and chaotic at the base of the Çubuklu (Fig. 9; Ç.5) and Dokanaklı (Fig. 9; Ç.6) regions and thinning laterally to the west in the Kalabak region (Fig. 9; Ç.7), where the thickness of these layers varies over the range 1–3 m. In the Çubukludağ region the subunit appears poorly sorted, clast supported and coarse grained (lithic fragment
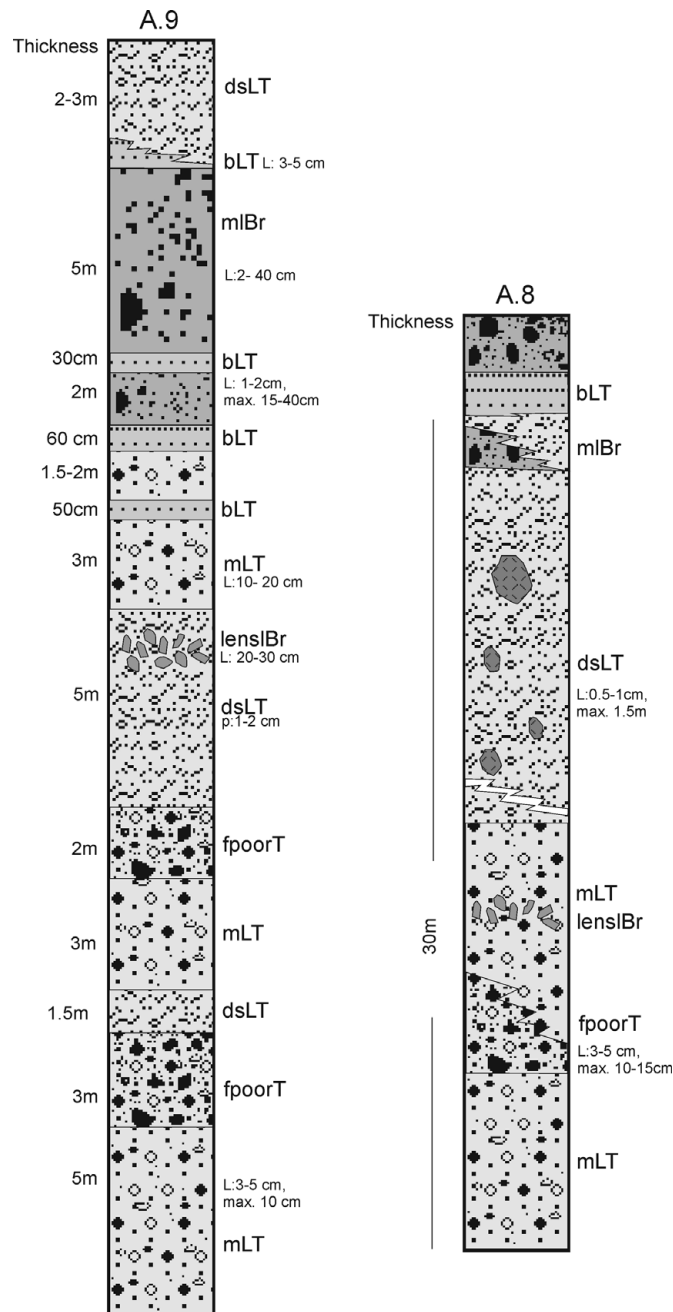
Figure 10. Measured stratigraphic sections from Çakmak Hill and Ayı Hill region in the central part of the Çubukludağ Graben. See Figure 4 for abbreviations and legends for the units. See the online Supplementary Material at http://journals.cambridge.org/geo for a full colour version of this figure.

sizes are on average 5–10 cm, maximum 40 cm) while at the base of the Çakmak Hill and in the Ayı region it is thick, coarse grained, fines poor and clast supported (Fig. 10; A.8 and A.9). It then becomes thinner and is seen as lenses in the Ayı Hill region (A.8 section in Fig. 10). In general the upper part is well sorted; the diameter of the lithic fragments is generally 0.5–1 cm with a maximum of 5 cm while pumice clasts are all 0.5–1 cm in diameter. This unit contains tube-shaped pumice fragments (20–40 cm in diameter) and covers the parallel-bedded pumices in the Kuner region (Fig. 6; K.2 section).

Subunit 2c can be seen at different levels within the pyroclastic section as thin layers with sharp and/or diffuse contacts (Fig. 9). It consists of thin-bedded lapilli tuff – tuff (bLT–bT) and massive and/or stratified ash tuff with ash and coated pellets (mTpel–mTcpel). The tuff – lapilli tuff consists of mainly fine to coarse ash and very small lithic and crystal fragments. Laterally continuous parallel bedding and/or lamination are the main characteristic features here. The average thickness is 20–40 cm but it does reach 1 m in some places, grading vertically or laterally into stratified and massive lapilli tuffs.

In some places, especially the Şaşal region, coarse sand and lapilli-sized massive tuffs contain abundant rounded and a few broken accretionary lapilli (Fig. 9; Ç.5; Fig. 13a). Well-developed, concentric, fine-ash laminations around an ash core are typical features. Some of the lapilli have double-layered accretionary
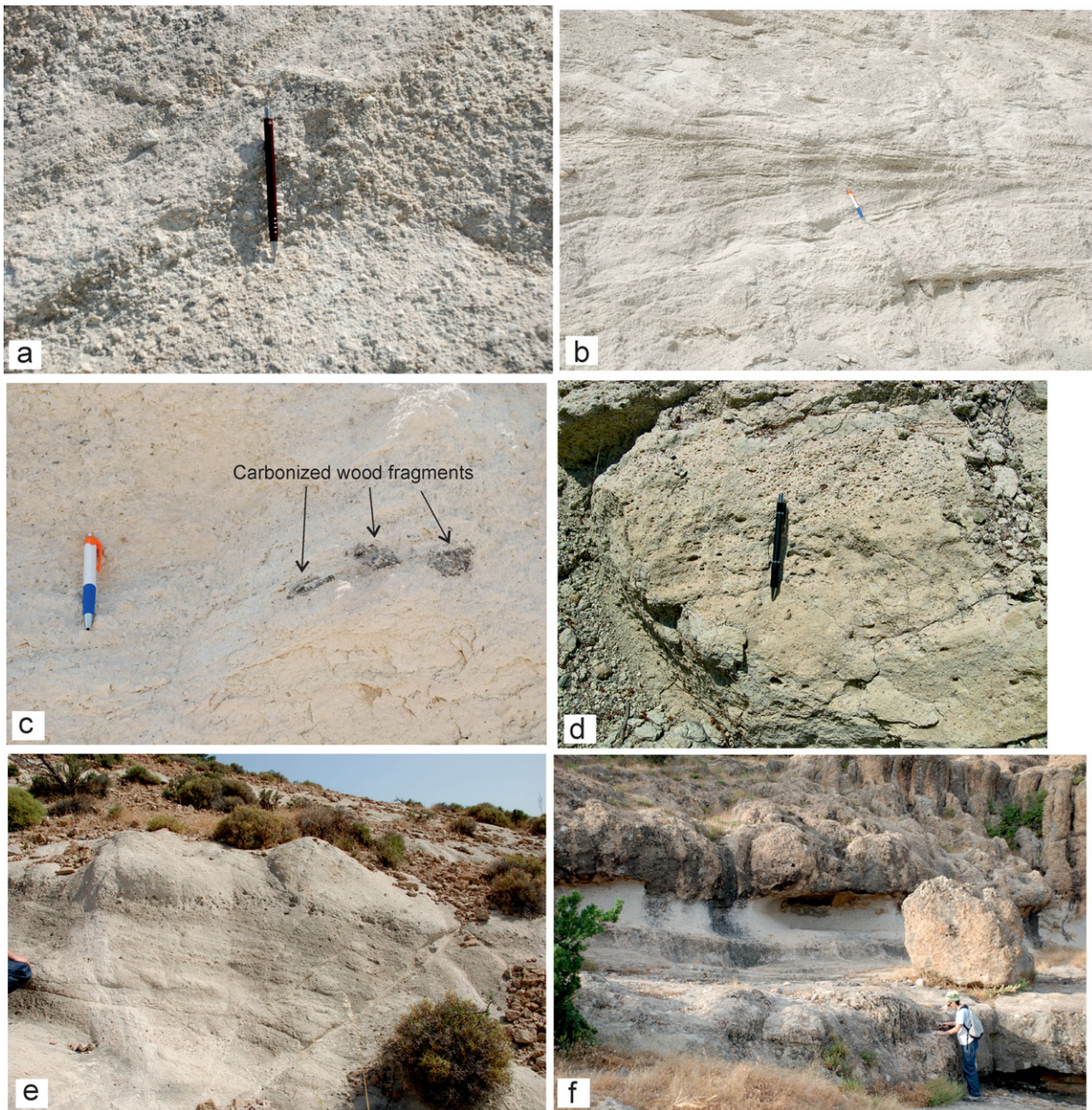
Figure 11. (Colour online) (a) General view of diffusely stratified lapilli tuff. (b) Low-angle truncations in the diffusely stratified tuff. (c) Carbonized wood fragments in the diffusely stratified lapilli tuff – tuff. (d) Different-sized partly elongated vesicules, rich in tuff – lapilli tuff. (e) Lithic-rich layers alternate with the diffusely stratified tuff. (f) General view of the alteration of the pumice-rich dsLT and mLT deposits.

rims (Fig. 13a) that are mostly sparsely scattered but clast supported in some layers. The thicknesses of these layers, containing concentric rim-type and cored accretionary lapilli (Schumacher & Schmincke, 1995), vary over the range 0.3–1 m. Abundant coated ash aggregates and ash pellets bearing massive tuff (mTpel–mTcpel) layers are seen in the middle and upper levels of the Kalabak region in Ç.7 section (Fig. 9), alternating with the dsLT and mLT. Lithic fragments are rarely seen; those that are seen vary greatly in size over the range 1–12 cm (Fig. 13b, c). The top of the section, composed of well-sorted thinly bedded pellet-rich layers (Fig. 13d, e), is widespread and reaches 0.5–2 m in thickness although it becomes much thicker (5 m) in the west of this section.

3.b.2.b. Interpretation

Unit 2 is a typical non-welded ignimbrite composed of poorly sorted, diffusely stratified, tuff – lapilli tuff (sLT–sT) and massive lapilli tuff – tuff (mLT–mT). The units pass into one another gradually across a few metres and/or alternate as different thickness layers. Sorting varies from sorted to poorly sorted with fine ash to lapilli blocks. Relatively well-sorted areas are indicators that particle segregation is locally efficient. Here, the pumice particles range in size greatly from fine ash to block, being derived from initial explosive fragmentation and further broken and abraded during transport. The lithic-breccia-rich layers and lobes indicate the accumulation and gravitational collapse of the lithic materials in the flow boundary
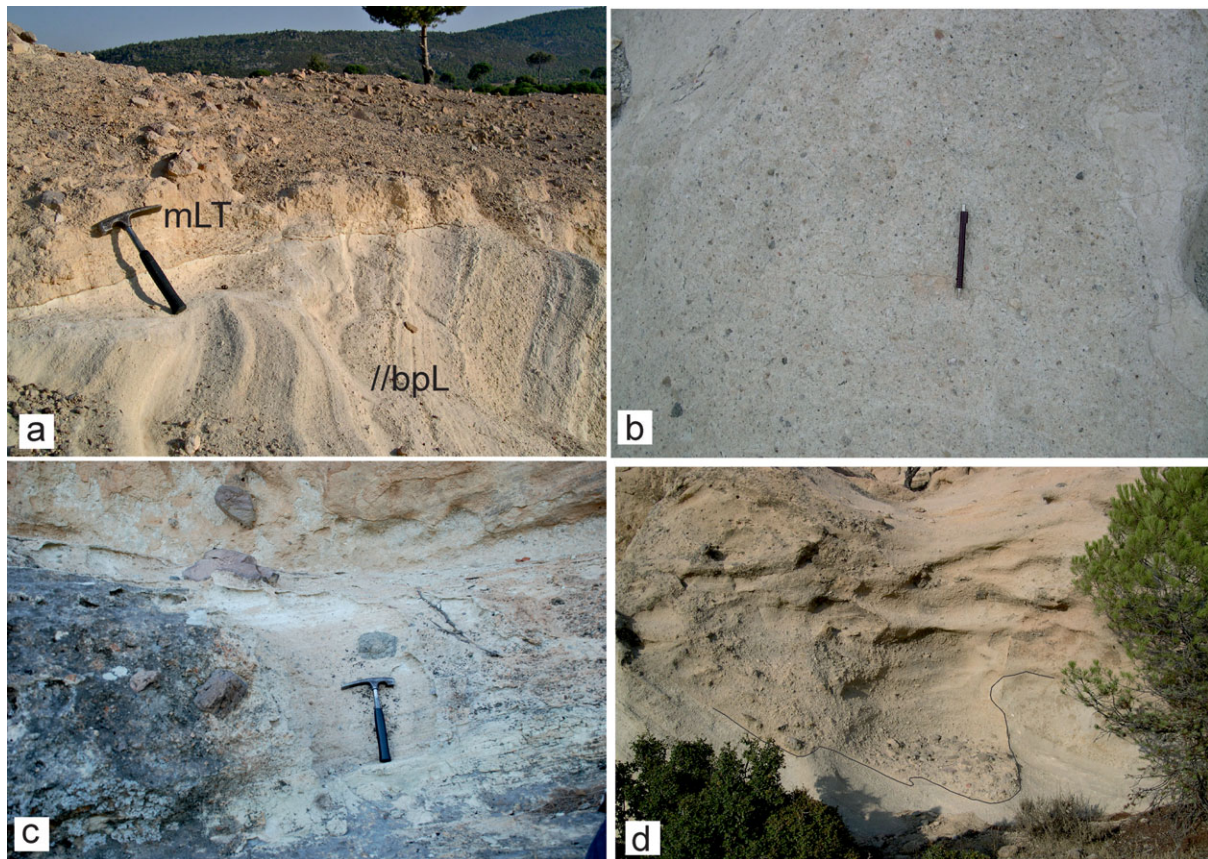
Figures 12. (Colour online) (a) Chaotic-massive lapilli tuff with lithic fragments covers the parallel-bedded pumice lapilli tuff. Block size varies over the range 2–20 cm in diameter. Matrix is composed of ash and pumice fragments. (b) General views of the massive textures of the massive lapilli tuff. (c) Rare lithic fragments are semi-rounded to angular and 30 cm in diameter in some layers. (d) Lithic breccia-rich lobes in the massive lapilli tuff which represents irregular contact.

zones. The presence of vesiculated ash tuffs indicate a trapped gas phase during hot pyroclastic flow (Fisher & Schmincke, 1984; Rosi, 1992). In addition, the elongated form of the vesicles suggests deposition during flow.

The presence of more accidental lithic fragments such as schists and sedimentary rocks together with the more massive structure-less, thick and poorly sorted deposits of the Şaşal domain may indicate their location at an intermediate distance from the vent. Branney & Kokelaar (2002) explained that diffuse-stratified lithofacies are deposited when flow-boundary zone conditions (i.e. the particle concentration and shear gradients) are somewhere between fluid escape-dominated and traction-dominated flow-boundary zones, depositing mLT and dsLT, respectively. Transitions between diffusely stratified and massive ash tuff – lapilli tuff indicates the changing conditions of a pyroclastic density current through time and space. The granular fluid-based PDC would have caused the massive part of the deposit (Branney & Kokelaar, 2002). The weakening of turbulence would have resulted in grain segregation within the PDC and the settling of large particles.

As stated earlier, the composition of subunit 2c is mainly fine to coarse ash. Together with the thin bedding and lateral persistence of each bed, this indicates that it is derived from pyroclastic fallout and/or ash-rich PDC. Despite examination of the ash fall deposits, we were unable to establish whether they resulted from a phreatomagmatic eruption plume or a co-ignimbrite plume. An abundance of accretionary lapilli in the Şaşal village sections are convincing evidence of its wet pyroclastic environment (moist deposition <100 °C) and identifies the boundary of the area affected by the phreatomagmatic eruption. In the Kalabak region (Fig. 9; Ç.7) well-sorted and parallel-bedded ash tuff and ash-coated pellet-rich layers could be classified as 'pellet fall layers' as proposed by Brown *et al.* (2010) (Fig. 13d, e). The lithological and stratigraphical features might be part of the deposits from the sustained PDC, which were the ash aggregates in the co-ignimbrite plume. The basal massive parts represent the transition zone between the mLT and ash pellets; the upper parts indicate dropped ash pellets from a co-ignimbrite ash plume.

The features outlined above, the presence of vesicles in tuff, accretionary lapilli and ash pellets and the fine grain-size of the tuffs are characteristic of moist deposition of the stratified tuffs (Branney & Kokelaar, 2002). Accretionary lapilli commonly form in steam-rich, phreatomagmatic eruption columns or in convection of the pyroclastic surge cloud when solid particles pick up sticky wet ash (Self & Sparks, 1978;
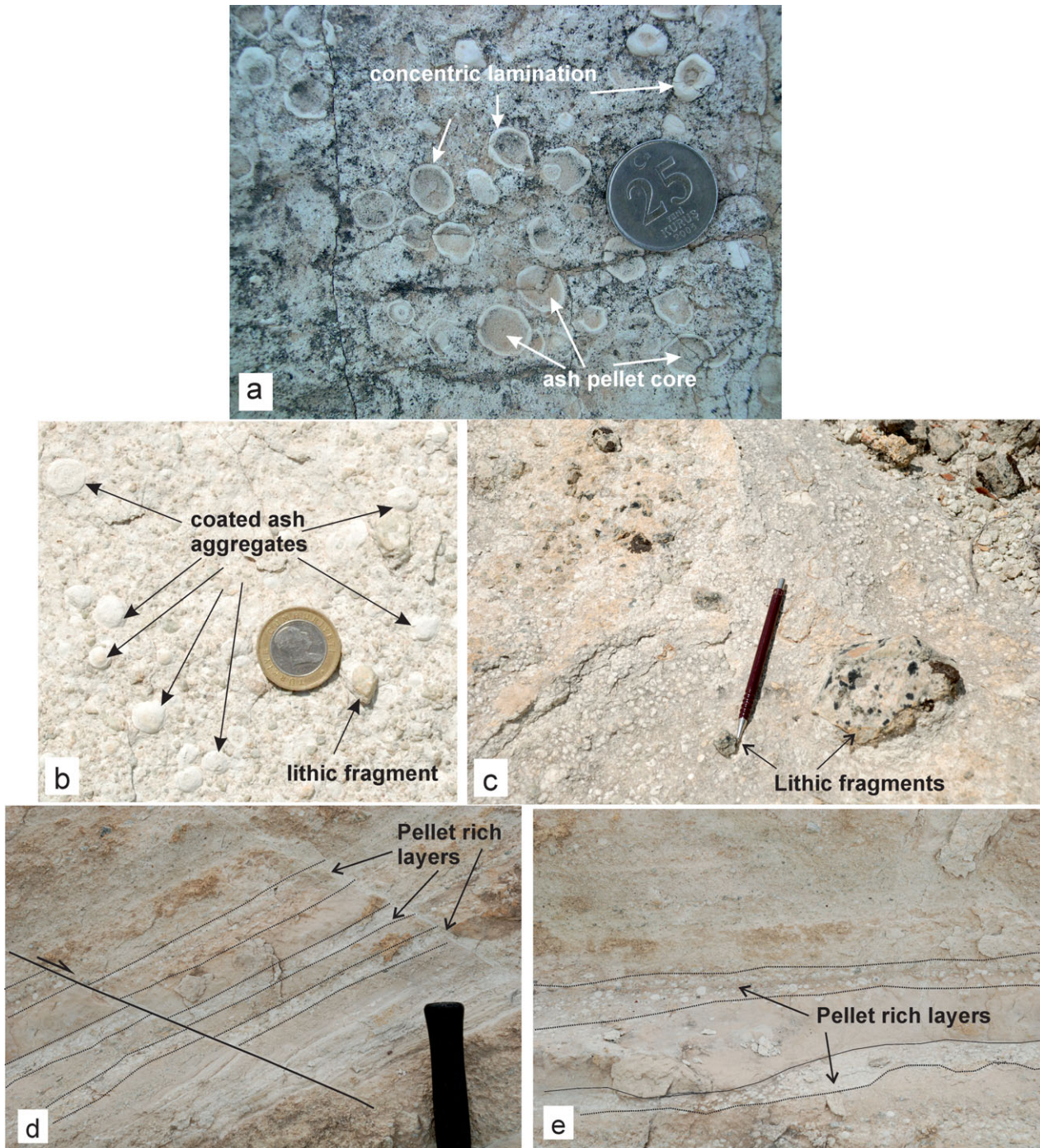
Figures 13. (Colour online) (a) Rim-type accretionary lapilli-rich pumice and ash deposits around the Şaşal village (coin diameter is 21.5 mm). (b) Coated ash aggregates and ash pellets bearing massive tuff (mTpel–mTcpel). (c) Rarely seen coarse lithic fragments (10–12 cm). (d, e) General view of ash-pellet-rich thinly bedded tuff.

Waitt & Dzurisin, 1981). Brown *et al*. (2010) proposed that rim-type accretionary lapilli are most common near the central part of a PDC. The ash particles were accreted and fell down shortly after the emplacement of the ash-laden PDCs. Although subunits 2a and 2b have a chaotic texture, 2c represents very noticeable bedding structures suggestive of a marker layer, indicating the centre of the PDCs.

All the lithological and structural features we examined are those of a non-welded ignimbrite and imply they were generated by an extensive PDC.

The presence of well-formed agglomerations such as accretionary lapilli and ash pellets and the non-welded character of unit 2 indicate a low-temperature emplacement of the deposits.

3.b.3. Unit 3

3.b.3.a. Description

The dominant lithology we found here is coarse-grained poorly sorted massive lithic breccia (mlBr) which is common in the northern part of the Çakmak
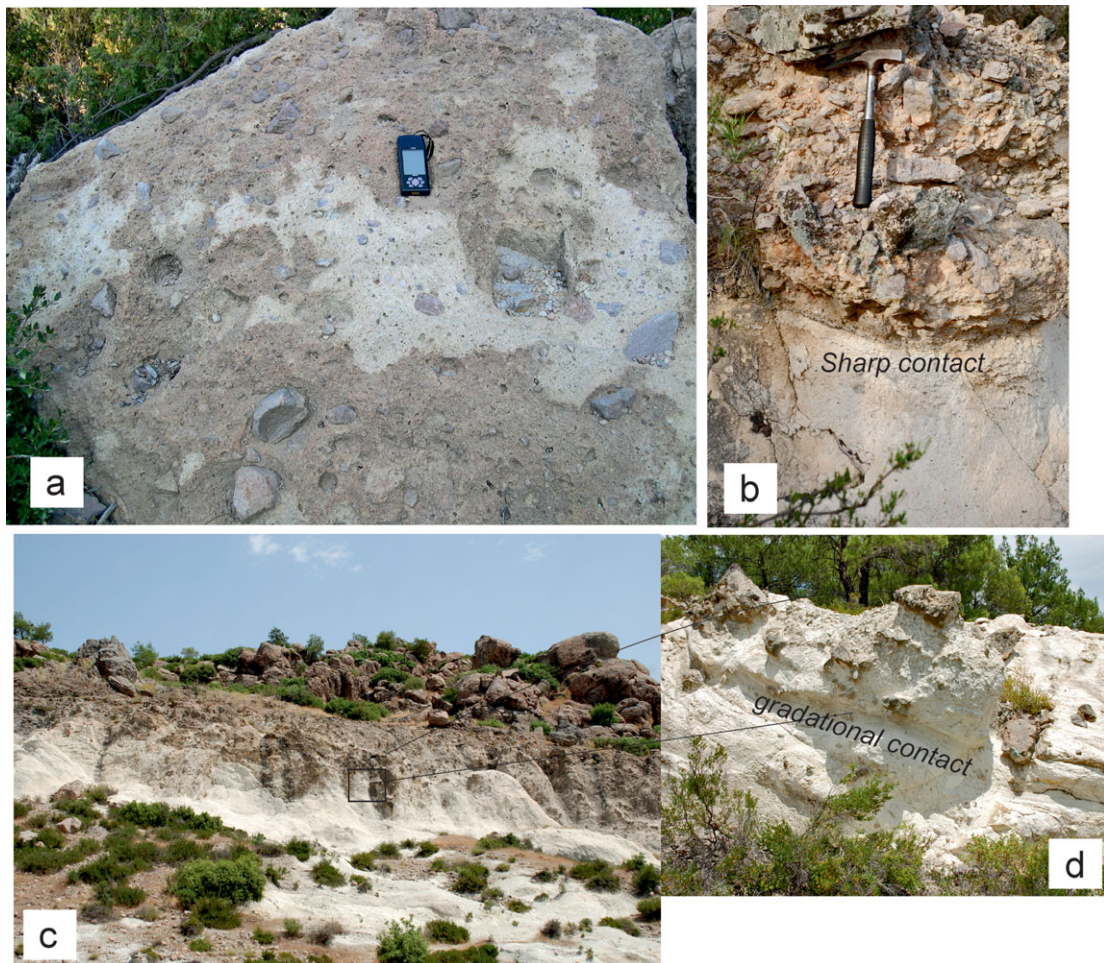
Figure 14. (Colour online) (a) General view of massive lithic breccia with perlite and rhyolite fragments (3–5 cm, maximum 15 cm) embedded in an ash-pumice matrix. (b) Clast-supported massive lithic breccia blocks are angular to sub-angular, perlitic and rhyolitic in composition. (c) General view of the matrix-supported flow deposits. (d) Closer view of the gradational contact.

Hill, Kalabak Hill and Şaşal regions (Figs 6, 9, 10). The Ayı Hill, Dokanaklı and Çubuklu regions commonly grade laterally and vertically into mLT of 1–2 m thickness, with alternate layers of diffuse-stratified tuff (dsLT) and massive lapilli tuff (mLT) (Fig. 9).

Despite the very thick (c. 1 m) nearly planar bedding observed in some places, the deposits are typically poorly sorted, slightly cemented and massive and with internally chaotic structures. The unit contains lithic blocks derived from cognate materials such as perlitic obsidian and rhyolite; accidental fragments, including chert, schist and sandstone, are rarely present.

We observed that the average fragment size is 10–15 cm, although in extreme cases it may be as small as 1–2 cm or as large as 40 cm in size (Fig. 14a). Blocks are generally slightly rounded and sub-angular in shape. The grain size and sorting are variable laterally and vertically in the succession. The matrix is composed of medium to coarse ash and pumice fragments. We have classified this unit as either matrix-to-clast supported, lithic-rich tuff breccias or clast-supported lithic fragment dominated breccias (Fig. 14a, b) due to the variable conditions of the matrix and clast.

In the Çakmak Hill, this thick unit is commonly intercalated with thin to very thinly bedded or laminated (30–60 cm) fine lapilli tuff (bLT) and medium- to fine-grained tuffs. Their contacts between mlBr and other units (dsLT and mLT) are gradational in the Şaşal and Dokanaklı region, but sharp in Kalabak region in section Ç.7 (Fig. 14b, c, d).

3.b.3.b. Interpretation

The contents of deposits (ash, pumice and lithic fragments) vary laterally and vertically with location. The massive lithic breccia is widespread in the Çakmak and Çubuklu Hill region and appears as 2–5 m thick layers with other deposits. These types of chaotic flow deposits can be produced from magmatic and/or phreatomagmatic eruptions (Cas & Wright, 1987). The lithological properties and structural features of the blocky deposits are similar to magmatic eruption products such as those of eruption column and/or lava dome collapse. The energy and extent of fragmentation is very intense in the types of flows which accumulate around the vents. It is clear to us that these coarse clastic-rich clast-supported flow deposits are the source region or eruption centre of the volcanoes.

The presence of juvenile glass (perlitic) fragments of different size and shapes and vesicles suggests that there has been fragmentation of an inhomogeneous magma and/or recycling of clasts as a result of repeated explosions (Nemeth & White, 2003). The different types of accidental lithic clasts such as metamorphic or sedimentary rocks may reveal that there were subsurface explosions and/or unstable conduits during eruptions (Nemeth & White, 2003). The ungraded, non- or weakly bedded and unsorted texture that characterizes this facies association is also consistent with primary pyroclastic deposition of the facies.

The eruptions are inferred to have dispersed material excavated by shallow subsurface explosions that created, or took place under, relatively open vent conditions. All these blocky units are produced by PDCs and form a coarse ignimbritic facies. Branney & Kokelaar (2002) proposed that lithic breccias are deposited through the lower flow boundary of a PDC. The lithological and textural variations in the deposits result from variation of flow-boundary zone conditions of PDCs. They are basically interpreted as a coarse equivalent of the mLT and called 'proximal lithic breccia' by Branney & Kokelaar (2002). These types of mlBr and mLT intercalations are seen very regularly in the Dokanaklı, Kalabak and Çakmak sections. Their deposition from high-concentration flow-boundary zones of pumiceous density currents is indicated by their rapid gradations into normal pumiceous ignimbrite (mLT). The composition of juvenile fragments and pumiceous matrix with variable thickness, geographic distribution, intergradations and/or transitions with dsLT and mLT all indicate that mlBr is a proximal deposit of the ignimbrites.

3.b.4. Lateral and vertical distribution of the pyroclastic units

All the vertical facies sequences in Kuner ignimbrite consist of roughly three distinct layers of fine-grained lower (unit 1), massive to stratified middle (unit 2) and coarse-grained upper units (unit 3) (Fig. 3).

Considering all structural and lithological features of the pyroclastic succession, we conclude that the Çubukludağ region (sections Ç.4–Ç.7) and Ayı region (sections A.8–A.9) were proximal regions near the vent. The upper parts of these sections are coarse grained, disorganized and massive facies (unit 3; mlBr) while the lower parts include widespread unit 2 deposits. Most deposits in the Kuner region are fairly fine grained (unit 1).

Although deposits within units 2 and 3 are coarse-grained and massive, unit 1 (1a and 1b) shows traction structures and parallel stratification, demonstrating progressive change from proximal to distal regions. We conclude from this that the deposits of unit 2 and 3 transform into the crudely stratified layers of subunits 1a and 1b down current. Particle concentration also decreases down current with a progressive increase in tractional processes as recorded in the Suwolbong tuff in Korea (Sohn & Chough, 1989).

Unit 2 in the centre of the Çubukludağ Graben is the thickest and most widespread of the succession. It passes laterally into subunit 1b before thinning through the NE part of the graben. These deposits also pass continuously into subunit 1a further NE within the graben. The irregular bedforms and small-scale faults are due to the soft sediment deformations caused by slumping and remobilization of material on the steeply sloping vent margins. Dunes and cross-bedding are typical structures in water-lain sediments deposited in turbulent environments. U-shaped erosion channels are the products of carving by later currents into the earlier deposits. The ash-pumice deposit of subunit 1b with its traction structures is typical of PDC-derived ignimbrites. The average thickness of the sand-wave bedding set increases from sections of K.3–K.2 areas to K.1 in the Kuner refion (Fig. 6). Dunes and cross-bedding indicate that the current direction was northward (N 5–50° W and NE). The trend and plunge of the axes of close folds are aligned N–S. The massive and diffuse-stratified ash and lapilli tuffs of unit 2 are a vertical continuation of unit 1 and also intercalated with them.

4. Lavas

4.a. Description

The main products of the Cumaovası volcanic rocks are lava flows and related flow breccias which were derived from single and/or multiple dome complexes and fissure eruptions. The rhyolitic domes are widely developed and aligned along the NE-trending faults that make up the Çubukludağ Graben (Figs 2, 15). They are small and distinct dome-shaped hills which have nearly symmetrical slopes. The most significant features are their circular forms in map view and flow foliations, which radiate away from the hills and commonly display subvertical attitudes near the eruption centres.

Domes of the Cumaovası volcanic rocks are mainly coulee and rarely spiny type (Fink & Anderson, 2000) (Fig. 16a, b). They appear in various sizes, implying the development of multi-vent volcanism. The biggest single domes are the Dededağ and Dikmen mountains which are *c.* 1.5 km in diameter; the smallest has a diameter of only 300 m (Orta Hill) (Fig. 16a). The most common lithology of the Dededağ and Dikmen domes is foliated stony rhyolites (Fig. 16c). Rocks from the NE slope of the Dededağ show similarities to highly vesiculated ignimbrite-like deposits (Fig. 16d). The unit, which flowed out NE-wards, is composed of pumice (0.5–2 cm), very rare lithic fragments and a pink-beige glassy matrix.

Temese Mt is a dome complex (clustered domes) which consists of two domes (each 1 km in diameter) with a vent from which the fissure eruption occurred (Fig. 15). The main lithologies here are stony rhyolite with pumiceous and spherulitic rhyolite intercalated with massive lithic breccias and ash tuff and flow breccias. Stony rhyolite forms the core of the domes
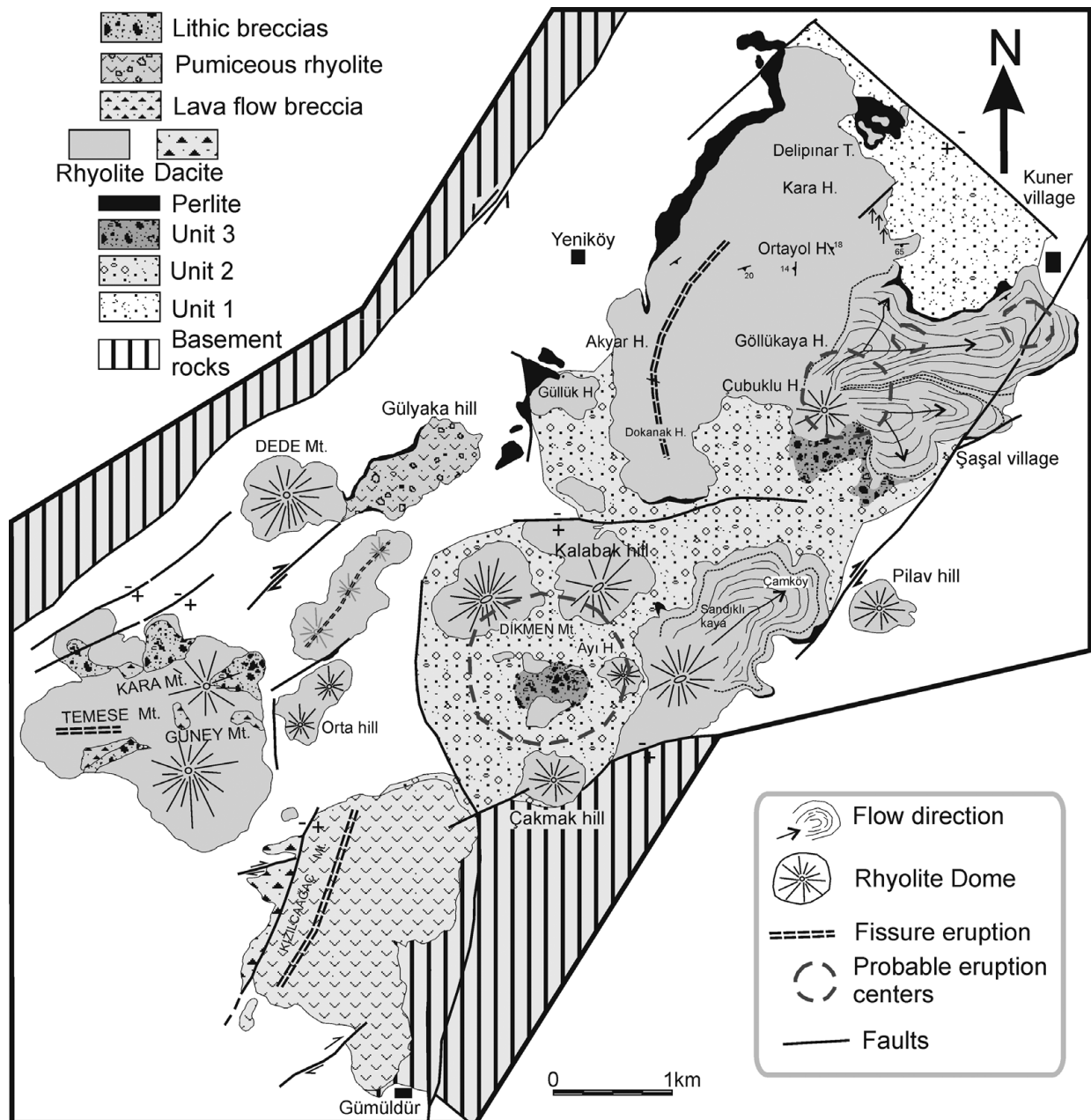
Figure 15. Simplified map of the Cumaovası volcanic rocks, showing the distribution of the pyroclastic units, silicic lava flows and domes, and relationships with the faults. Additionally, the flow directions and location of the fissure eruptions are also marked on this map. See the online Supplementary Material at http://journals.cambridge.org/geo for a full colour version of this figure.

(Fig. 16c). A pumiceous vesiculated zone and brecciated parts form the carapace of the domes (Fig. 16d). The existence of pumice-rich zones indicates volatile migration between the rhyolite (main body) and the glassy carapace. Typically the fissures are orientated in a NE–SW direction and are present around the Kızılcaağaç area in the south and Akyar in the northern part of the Çubukludag Graben (Figs 2, 15). The former is dacitic while the latter is rhyolitic in composition. The lavas of Çubuklu Mt, classified as multi-lobed flows, are located in the eastern part of the graben. The two main lobes are NNE and SSE oriented, and flowed up to 4 km and 2.5 km away from the centre, respectively. Çamköy area also represents a lobed rhyolite flow that flowed 2 km in the NNE direction. The extrusion of

the Temese and Dededağ domes together with the Kızılcaağaç fissure eruption probably began during the main phreatomagmatic eruptions and cut and/or covers the basement rocks. By contrast, the other domes are younger and flowed over the earlier pyroclastic deposits.

The lava eruptions that occurred within the entire Çubukludağ Graben are rhyolitic, rhyodacitic and dacitic in composition (Karacık et al. 2013). The most common lithologies are phenocryst-rich stony rhyolites, pumiceous rhyolite, aphyric obsidian and perlites. The typical rhyolite domes and lava lobes of the Cumaovası volcanic rocks have autobrecciated layers at the bottom and in the carapace due to a flow fragmentation. Microcrystalline stony rhyolite forms
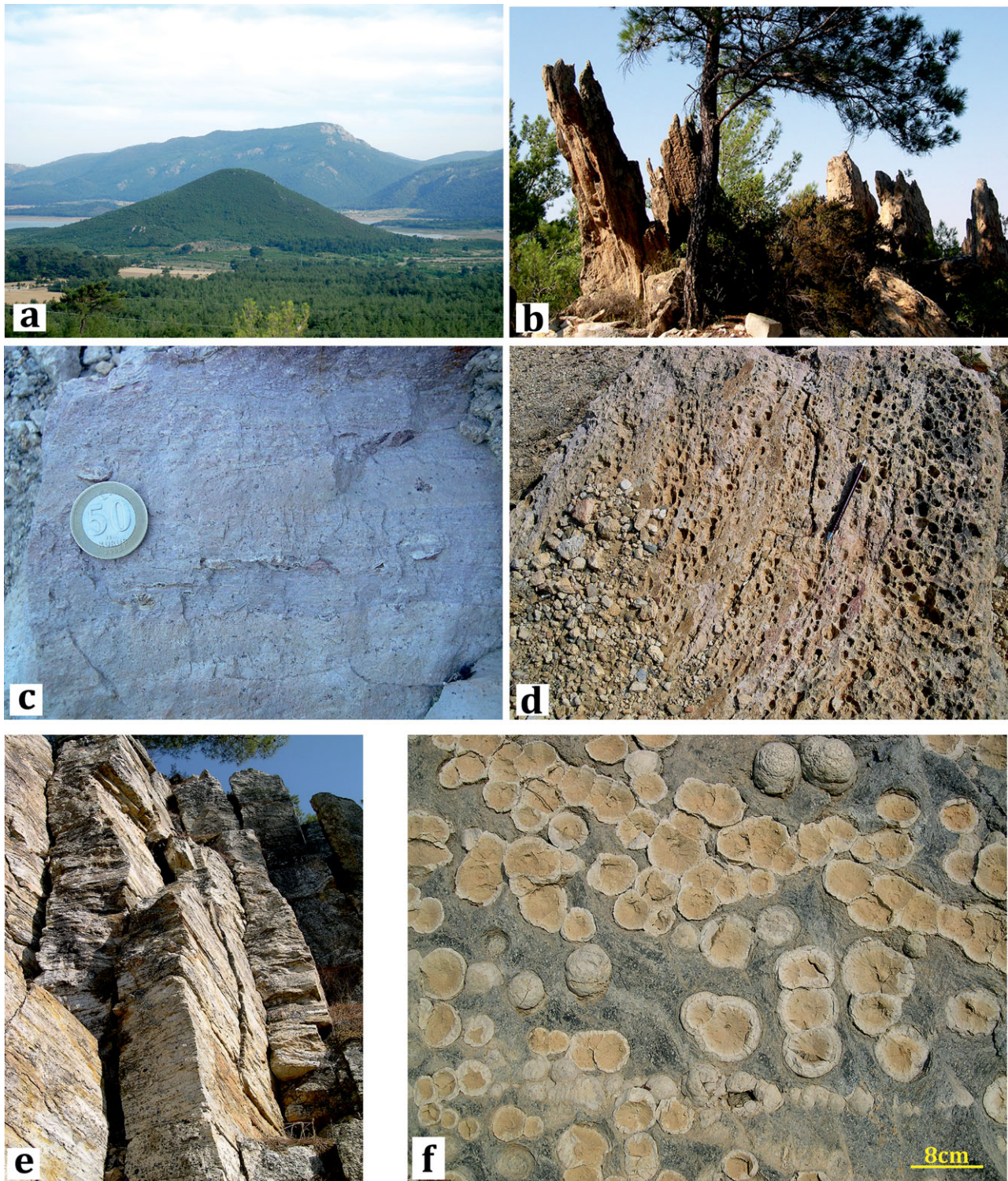
Figure 16. (Colour online) (a) General view of the Pilav dome. (b) Spiny-type rhyolitic lavas from Kalabak Hill. (c) Crystal-rich flow-banded stony rhyolite. (d) Vesiculated and flow-banded rhyolite. (e) General view of flow foliation and columnar cooling joints of the stony rhyolite. (f) Different-sized 'thundereggs' in the obsidian flow.

the core of the lava domes and lobes, indicating slow cooling. The stony rhyolites exhibit well-developed flow foliations and columnar cooling joints which are frequently intercalated with pumice tuff and flow breccias (Fig. 16e). Flow banding results from viscous flow of the magma prior to cooling of the glass. Our petrographic examinations revealed that the stony rhyolites consist of resorbed quartz, sanidine, plagioclase and biotite phenocrysts with matrix which can be felsitic, microlithic, granophyric and glassy. Vitrophyric and spherulitic textures are common.

Pumiceous rhyolite contains different-sized pumice and vesicles which are widespread around the carapace of the Güney and Karakaya domes and Gülyaka Hill. While the original pumices were preserved in the centre of the flows, they became fragmented by

movement within the upper and lower parts of the lava flows. Pumice-rich rhyolitic lavas alternate with co-eruptive pumice-rich blocky flow deposits in some places. They consist of rhyolite and obsidian fragments (5–40 cm) together with the coarse pumice (3–5 cm). There are spherulites, lithophysal cavities (average 3–5 cm, maximum 20 cm) occurring as banded layers and scattered irregularly within the rhyolites. There are also thin bands of opal as well as spheroidal nodules in fracture zones in the dacitic lavas.

Aphyric obsidian, perlite and related flow breccias are extensively present at the base of the rhyolitic lavas in the north around the Güllük, Yeniköy and Kuner areas (Figs 2, 15). The perlitic breccias are characterized by clast-supported, poorly sorted and non-graded deposits and have a thickness of c. 5 m on average, reaching 10 m in some places. The obsidian and perlites have a similar average thickness but reach up to 15–20 m, especially in the Yeniköy area. Thin (centimetre-scale), white, lithophysae-rich zones form a banded texture in obsidians and perlites (Fig. 16f). Perlites are a pale–dark-grey banded crystal-poor rock. They developed a thick glassy carapace due to the higher cooling rates of these vitrophyric-phase products.

4.b. Interpretation

Highly vesiculated rhyolite such as pumiceous-rich rhyolite around the Temese dome complexes and vesiculated ignimbrite-like deposits in Gülyaka Hill (eastern part of the Dededağ dome) are interpreted as the late-stage products of pyroclastic eruptions (Fink, 1983). After violent eruptions, the remaining volatile-rich magma reaches the surface as highly inflated pumiceous lavas and passes gradually into ordinary lava flows. These types of lithologies such as pumice-rich and vesiculated rhyolites intercalated with pyroclastic flow deposits in some restricted places in the Cumaovası volcanic rocks.

Spherulite-bearing lavas indicate devitrification of unstable glassy lavas similar to snowflakes, which have been described as 'secondary vesiculation' (Stevenson et al. 1994). The type and size of the spherulites depends on the temperature, pressure, time and fluid composition of the lavas (Lofgren, 1970, 1971a, b). Opal nodules are composed mainly of massy opal-CT and rarely lussatite with opal-A in voids as pore-filling minerals to form gem-quality fire opals (Karacık et al. 2011). Different-sized nodules are also common in the rhyolitic lavas which are known as 'thundereggs' (Shaub, 1979; Kshirsagar et al. 2012). 'Thundereggs' are spherical nodules in glassy silicic rocks, which lack the radial structure of spherulites. They contain secondary silica in their cores and fractures.

Perlitic alteration of the glassy lavas is important evidence for water interaction with the lava lobe margin. Such perlite presence indicates that the obsidian occurs as a flow, containing a flow-brecciated basal layer. During the vent eruption, but after the

obsidian had flowed, the remaining magma cooled and crystallized. The eruption of this magma as a crystal-rich rhyolite flow, capping the vent, forms the rhyolite domes. The final stage of volcanism is the emplacement of rhyolite domes with nearly all the vents plugged by the stony rhyolitic lavas.

The different lithological properties of the lavas are a result of variations within the crystal content, crystallization temperature and crystallization time-sequence of the Cumaovası magmas.

5. Discussion

The Cumaovası volcanic succession is a typical example of a silicic dome-related pyroclastic product and its stratigraphic features clearly record the contemporaneous phreatomagmatic and magmatic activity of independent and neighbouring vents. Extensive fine ash-rich deposits of the Kuner region might have been produced by vent-opening phreatomagmatic eruptions (unit 1). The fine-grained stratified dune-bedded deposits display features very similar to the base surge deposits which are well described by Fisher & Schmincke (1984) and Chough & Sohn (1990). On the other hand, more recent studies have described the same deposits as pyroclastic density current (PDC) deposits (Branney & Kokelaar, 2002; Francis & Oppenheimer, 2004). PDC deposits result from several separate surges and often form the walls of tuff rings and maars. They rarely reach more than 5–6 km from the vent. Hydro-volcanically derived PDCs are often moist and sticky because of the condensed steam. Deposits within units 2 and 3 cropping out in the central parts of Çubukludağ Graben are likely to be PDC-derived deposits.

Lateral and vertical facies variation and lithological properties are outlined in Figure 3. In the following paragraphs, we present and discuss the evidence for the abovementioned volcanic evolution.

The Kuner ignimbrite is made up of abundant pumice and irregular juvenile lithic fragments mostly 0.5–2 cm in diameter, embedded in lapilli and ash matrix. Depositional structures such as cross-lamination and variable geometries of sand-wave forms show inverse gradation of the components within individual beds. These typical structures indicate that the deposit originated as a wet base surge, which was probably produced by explosive fragmentation of the host rock by the phreatomagmatic eruptions. The fine laminations seen in unit 1 deposits offer an excellent opportunity to identify small displacements and/or slope failure accomplished by syndepositional normal faulting. Accretionary lapilli, ash pellets and soft sediment deformation features also suggest condensed water droplets in the transporting currents. These reflect deposition very near to the vents, before eruptive water vapour had begun to condense during flow.

Most of the fine-grained thin layers of tuff deposits (subunit 1a) which are intercalated with the cross-stratified deposits (subunit 1b) may be interpreted

as both pyroclastic surge and pyroclastic fallout (Wohletz & Sheridan, 1979; Houghton *et al.* 2000; Tait *et al.* 2009). It is very difficult to differentiate these mechanisms on the basis of the grain size and sorting characteristics (Wohletz & Sheridan, 1979; Houghton *et al.* 2000; Tait *et al.* 2009). The only difference between the two is the lack of highly turbulent density current-derived structures in the fine-grained tuff units. Moving actively, PDCs and related ash clouds produce co-surge ash horizons as discrete horizons within the traction-dominated deposits. The occurrence of PDCs and co-genetic fall-derived deposits are very common in the tuff ring and tuff cone pyroclastic sequences (Tait *et al.* 2009).

Deposits within unit 2 consist mainly of stratified and/or massive lapilli tuff with lithic fragments. These thick, massive, chaotic, poorly sorted, non-welded deposits were derived from high-particle concentration pyroclastic flows. The components are lava fragments, pumices and accidental lithic clasts composed of the metamorphic and sedimentary fragments derived from the basement units. The non-welded nature of this unit can be explained in two ways: (1) the phreatomagmatic eruptions were not hot enough for the welding and, in this condition, interaction with external water reduces the emplacement temperature of the deposits; and (2) because of the small volume eruptions there was not enough heat for the generation of welding in the pumiceous deposits, even though welding is common in normal PDCs (Ellis & Branney, 2010). The presence of abundant ash aggregates is an indicator for phreatomagmatic eruption and moist eruption plumes. The fine-grained thinly bedded accretionary lapilli-rich tuff layers, the only ordered and continuous layer as a marker, indicate the approximate site of the central part of the density currents.

The massive lithic breccia deposits (unit 3) are very small volumetrically and entirely composed of juvenile (rhyolitic and perlitic) fragments which cover all of the previous unit. These basic features may indicate a gravity-driven collapse mechanism of a lava dome. Alternatively, these deposits might have been generated directly from vents where the eruption column only arose a small height above the vent and instantly collapsed without having generated a high eruption column (Cas & Wright, 1987). Although there is no morphological evidence indicating the eruption centre in the Çubukludağ Graben, massive lithic breccia-rich deposits (unit 3) might represent the vent areas (Figs 2, 15).

Proximal-to-distal facies changes indicate changes in flow-boundary conditions moving away from the source of the PDC (Branney & Kokelaar, 2002). In the Kuner ignimbrite there are different pyroclastic units that produced several repeated PDCs. In general, pumice-rich ash deposits formed at the base and were overlain by mLT and dsT alternations up to the mlBr. This type of vertical succession displays similarities to vertical sections through the waxing (PDC) flow which was described by Branney & Kokelaar (2002). The

Kuner ignimbrite is non-welded and has nearly all the different units and subunits expected in a PDC.

The eruption styles of the silicic lavas are controlled by the volcano-morphology and structure such as cone-forming (fallout-dominated) to ring-forming (surge-dominated). The resulting volcanic edifices consist of multiple rim beds of partial tuff rings and/or tuff cones commonly with non-circular morphologies. The ring-versus-cone morphology of the hydromagmatic volcanoes is dependent on eruption style, interaction between magma and water, lithology and the mechanical properties of conduit wall rock and vent geometry (Sohn & Park, 2005). There is no clear circular morphology formed by pyroclastic products in the Cumaovası region. The reason for this may be either that (1) the eruptions occurred from linear vents or (2) the eruptions occurred on a soft substrate. Where hydromagmatic eruptions are situated on unstable sedimentary substrates such as those described on Jehu Island, Korea (Sohn & Park, 2005), lateral vent migration is a very important phenomenon. The substrate in which an eruption took place can have a significant effect on the surface morphology, for example as circular morphologies in hard substrate versus irregular non-circular morphologies in soft substrate settings (Sohn & Park, 2005). Deposits within unit 1 of the Kuner ignimbrite are found on the intersections of the NE–SW- and NW–SE-trending main fault system and also on the soft lacustrine deposits, which form a significant part of the basement rock. For this reason, the lack of clearly developed ring morphology in the region may be explained by the tectonic setting and patterns characterizing the region during the eruptions and the lithological properties (such as soft lacustrine deposits) of the basement rocks in the Kuner region.

In conclusion, the NE–SW-trending Çubukludağ Basin was filled by continental red-beds (the Ürkmez Formation) and lacustrine sediments (the Yeniköy Formation) during the late Early Miocene period (Genç *et al.* 2001; Uzel & Sözbilir, 2008). The former is dominant in the southern areas while the latter is widespread in the NE parts of the graben (see Fig. 2). The lacustrine sediments of the Yeniköy Formation pass laterally and vertically into the volcanic-sedimentary transitional deposits (VSTD). The widespread pyroclastic deposits are cut and covered by rhyolite and dacitic lava domes and flows.

Considering this distribution and the stratigraphic relationships between the lavas and pyroclastic deposits, we propose that the volcanic activity began with phreatomagmatic eruptions, producing the different units of the Kuner ignimbrite in the NE part of the region and then propagated in a SW direction controlled by the fractures zone(s). These deposits pass laterally and horizontally into coarse-grained pyroclastic deposits which were derived from discrete vents by violent eruptions and/or related column collapse. The rhyolitic domes and fissures eruptions also followed this weakness zone.

6. Conclusion

The Cumaovası volcanic rocks form an upper part of the Çubukludağ Graben infill, which reflects an extension-related crustal fissure-fracture zone within the basin. Lake deposits of the Yeniköy Formation represent the upper parts of the sedimentary infill of the basin that were covered by pyroclastic rocks of phreatomagmatic origin, from the early eruptive phase of volcanic activity. Volcanic-sedimentary transitional deposits (VSTD) in the central part of the graben clearly indicate this genetic connection.

The main products of phreatomagmatic eruptions are fine laminated ash tuff (subunit 1b) with a main body of pyroclastic density currents that exhibit traction structures in fine ash-lapilli-rich deposits (subunit 1b) followed by massive diffusely stratified ash-lapilli deposits (unit 2). These deposits display proximal flow characteristics and the former have distal surge characteristics.

Later magmatic eruptions may have been produced by column collapse event(s) to form coarse-grained massive lithic breccias (unit 3) in the central part of the graben (Figs 2, 14). Many of the fine-grained and laminated ash layers accompanying the pyroclastic deposits are interpreted as co-genetic fall deposits. The pyroclastic eruptions were followed by the extrusion of lava flows and emplacement of silicic domes (Figs 2, 14). The Cumaovası volcanic rocks have a linear distribution along the NE–SW-trending fault zone and many of the vents seem to have been located along fissures and to have fed nests of domes. Lavas may possibly have extruded simultaneously from neighbouring vents, suggesting multi-vent-type volcanism.

Phreatomagmatic eruptions of low-concentration highly mobile fine-grained pumiceous tuffs from discrete vents were followed by the largest explosive eruptions of the Cumaovası region, which originated in the central area around the Dikmen Mt and Kalabak and Ayı hills. The massive and diffusely stratified tuffs from PDCs were funnelled into the valleys around the many vents. It should be noted that, beside these main eruptions, small local phreatomagmatic explosions may have occurred. Examples of these are Temese Mt multi-domes and the inter-fingered pyroclastic flow deposits. These represent the volatile-rich evolved cap of the acidic magma chamber beneath the graben which erupted contemporaneously with the domes.

Silicic lava flows may be divided into two parts: (1) phenocrysts rich (stony rhyolite) and (2) nearly aphyric (i.e. obsidian-perlite). The initial product of the explosive eruptions was primarily an almost-aphyric magma. This was commonly followed by the phenocryst-rich magma that is both widespread and largest. Perlite occurrences observed beneath the rhyolitic lava flows indicate that water interacted with the lobe margins. Dykes rose from the magma chamber and intersected the ground surface, forming eruptive fissures. When explosive activity ceased, the crystal-rich lava effused from the fissures and formed the domes. The final stage was marked by effusive eruptions and extrusions of small rhyolite and dacite bodies. These appear to represent the final phases of the Cumaovası volcanism. In this extensional setting, fracturing and volcanism occur together and the volume of silicic lavas is greater than those of the pyroclastic deposits. For this reason, the Cumaovası volcanic rocks are a very good example for extensional-related silicic volcanism, such as that observed in the Snake River plain in Yellowstone, US, the Ramadas volcanic centre in Andean Puna and the Taupo volcanic zone in New Zealand (Brooker *et al.* 1993; Smith *et al.* 2005; Deering *et al.* 2008; Tait *et al.* 2009; Ellis & Branney 2010).

There are many active geothermal fields in the area, which contain numerous hot-water springs with comparatively high temperatures (Eşder & Şimşek, 1975). This hydrothermal activity may be related to the high heat flux due to the asthenospheric upwelling, the last product of rhyolitic volcanic activity.

References

AKARTUNA, M. 1962. İzmir-Torbalı-Seferihisar-Urla bölgesinin jeolojik etüdü. *İstanbul Üniversitesi Fen Fakültesi Monografileri* **18**, 18.

BAŞARIR, E. & KONUK, Y.T. 1981. Gümüldür yöresinin kristalin temeli ve allokton birimleri. *Bulletin of the Geological Society of Turkey* **24**, 1–6.

BLUTH, J. K. 2004. Syn-erutive incision of Koko Crater, Oahu, Hawaii by condensed steam and hot cohesive debris flows: a re-interpretation of the type locality of "surge-eroded U-shaped channels". Published thesis, Master of Science. University of Pittsburgh.

BORAY, A., AKAT, U., AKDENIZ, N., AKÇÖREN, Z., ÇAĞLAYAN, A., GÜNAY, E., KORKMAZER, B., ÖZTÜRK, E.M. & SAV, H. 1973. Menderes Masifinin güney kenarı boyunca bazı önemli sorunlar ve bunların muhtemel çözümleri. *Cumhuriyetin 50. Yılı Yerbilimleri Kongresi, Tebliğler*, Mineral Research and Exploration Institute of Turkey, Turkey, 11–20.

BORSI, S., FERRARA, G., INNOCENTI, F. & MAZZUOLI, R. 1972. Geochronology and petrology of recent volcanics in the Eastern Aegean Sea (West Anatolia and Lesvos Island). *Bulletin of Volcanology* **36**(3), 473–96.

BOZKURT, E., PARK, G. & WINCHESTER, J.A. 1993. Evidence against the core/cover interpretation of the southern sector of the Menderes massif, west Turkey. *Terra Nova* **5**, 445–51.

BRANNEY, M.J. & KOKELAAR, P. 2002. *Pyroclastic Density Currents and the Sedimentation of Ignimbrites*. Geological Society, London, Memoir **27**, pp. 143.

BROOKER, M.R., HOUGHTON, B.F., WILSON, C.J.N. & GAMBLE, J.A. 1993. Pyroclastic phase of a rhyolitic dome-building eruption: Puketarata tuff ring, Taupo Volcanic Zone, New Zealand. *Bulletin of Volcanology* **55**, 395–406.

BROWN, R.J., BRANNEY, M.J., MAHER, C. & DAVILA-HARRIS, P. 2010. Origin of accretionary lapilli within ground-hugging density currents: evidence from pyroclastic couplets on Tenerife. *GSA Bulletin* **122**, 305–20.

BROWN, R.J., KOKELAAR, B.P. & BRANNEY, M.J. 2007. Widespread transport of pyroclastic density current from a large silicic tuff ring: the Glaramara tuff, Scafell caldera, English Lake District, UK. *Sedimentology* **54**, 1163–89.

CAS, R.A.F. & WRIGHT, J.V. 1987. *Volcanic Successions Modern and Ancient: A Geological Approach to Processes, Products and Successions*. Unwin Hyman, London.

CHOUGH, S. K. & SOHN, Y.K. 1990. Depositional mechanics and sequences of base surges, Songaksan tuff ring, Cheju Island, Korea. *Sedimentology* **37**, 1115–35.

DEERING, C.D., COLEI, J.W. & VOGELI, T.A. 2008. A rhyolite compositional continuum governed by lower crustal source conditions in theTaupo Volcanic Zone, New Zealand. *Journal of Petrology* **49**(12), 2245–76.

DRAHOR, G. & BERGE, M.A. 2006. Geophysical investigations of the Seferihisar geothermal area, Western Anatolia, Turkey. *Geothermics* **35**, 302–20.

ELLIS, B. & BRANNEY, M.J. 2010. Silicic phreatomagmatism in the Snake River Plain: the Deadeye Member. *Bulletin of Volcanology* **72**, 1241–57.

ERDOĞAN, B. 1990. İzmir-Ankara zonu'nun, İzmir ile Seferihisar arasındaki bölgede stratigrafik özellikleri ve tektonik evrimi. *Türkiye Petrol Jeologları Derneği Bülteni* **2**(1), 1–20.

EŞDER, T. & ŞIMŞEK, Ş. 1975. Geology of Izmir (Seferihisar) geothermal area, Western Anatolia of Turkey: determination of reservoirs by means of gradient drilling. *In: Proceedings of the second UN Symposium on the Development and Use of Geothermal Resources*, San Francisco, pp. 349–61.

FINK, J.H. 1983. Structure and emplacement of a rhyolite obsidian flow: Little Glass Mountain, Medicine Lake Highland, Northern California. *Geological Society of America Bulletin* **94**, 362–80.

FINK, J.H. & ANDERSON, S.W. 2000. Lava domes and coolees. In *Encyclopedia of Volcanoes* (eds H. Sigurdsson, B.F. Houghton, S.R. McNutt, H. Rymer & J. Stix), pp. 307–19. Academic Press, San Diego.

FISHER, R.V. & SCHMINCKE, H.-U. 1984. *Pyroclastic Rocks*. Springer-Verlag, Berlin, 472 pp.

FRANCIS, P. & OPPENHEIMER, C. 2004. *Volcanoes*. Oxford University Press, Oxford.

GENÇ, Ş.C., ALTUNKAYNAK, Ş., KARACIK, Z., YAZMAN, M. & YILMAZ, Y. 2001. The Çubukludağ graben, south of İzmir: its tectonic significance in the Neogene geological evolution of the western Anatolia. *Geodinamica Acta* **14**(1/3), 45–55.

HELVACI, C., ERSOY, E.Y., SÖZBILIR, H., ERKÜL, F., SÜMER, Ö. & UZEL, B. 2009. Geochemistry and ^{40}Ar/^{39}Ar geochronology of Miocene volcanic rocks from the Karaburun Peninsula: implications for amphibole-bearing lithospheric mantle source, Western Anatolia. *Journal of Volcanology and Geothermal Research* **185**, 181–202.

HOUGHTON., B.F., WILSON, C.J.N. & PYLE, D.M. 2000. Pyroclastic fall deposits. In *Encyclopedia of Volcanoes* (eds H. Sigurdsson, B.F. Houghton, S.R. McNutt, H. Rymer & J. Stix), pp. 571–80. Academic Press, San Diego.

INNOCENTI, F. & MAZZUOLI, R. 1972. Petrology of the İzmir-Karaburun volcanic area (West Turkey). *Bulletin of Volcanology* **36**(1), 88–103.

JUSTET, L. & SPELL, T.L. 2001. Effusive eruptions from a large shallow magma chamber: the Bearhead Rhyolite, Jemez Volcanic Field, New Mexico. *Journal of Volcanology and Geothermal Research* **107**, 241–64.

KARACIK, Z., GENÇ, Ş.C., ESENLI, F. & GÖLLER, G. 2011. The Gümüldür fire opal: mode of occurrence and mineralogical aspects. *Turkish Journal of Earth Sciences* **20**, 99–114 .

KARACIK, Z., GENÇ, Ş.C. & GÜLMEZ, F. 2013. Petrochemical features of Miocene volcanism around the Çubukludağ graben and Karaburun peninsula, western Turkey: implications for crustal melting related silicic volcanism. *Journal of Asian Earth Sciences* **73**, 199–217.

KONUK, Y.T. 1977. Bornova Flişi'nin yaşı hakkında. *Ege Üniversitesi Fen Fakültesi Dergisi* **B**(1), 65–73.

KSHIRSAGAR, P.V., SHETH, H.C., SEAMAN, S.J., SHAIKH, B., MOHITE, P., GURAV, T. & CHANDRASEKHARAM, D. 2012. Spherulites and thundereggs from pitchstones of the Deccan Traps: geology, petrochemistry, and emplacement environments. *Bulletin of Volcanology* **74**, 559–77.

LOFGREN, G. 1970. Experimental devitrification rate of rhyolite glass. *Geological Society of American Bulletin* **81**, 553–60.

LOFGREN, G. 1971a. Experimentally produced devitrification textures in natural rhyolite glass. *Geological Society of America Bulletin* **82**, 553–60.

LOFGREN, G. 1971b. Spherulitic textures in glassy and crystalline rocks. *Journal of Geophysical Research* **76**, 5635–48.

LORENZ, V. 1974. Vesiculated tuffs and associated features. *Sedimentology* **21**, 273–91.

NEMETH, K. & WHITE, J.D.L. 2003. Reconstructing eruption processes of a Miocene monogenetic volcanic field from vent remnants: Waipiata Volcanic Field, South Island, New Zealand. *Journal of Volcanology and Geothermal Research* **124**, 1–21.

OCAKOĞLU, N., DEMIRBAĞ, E. & KUŞÇU, İ. 2004. Neotectonic structures in the area offshore of Alaçatı, Doğanbey, and Kuşadası (western Turkey): evidence of strike-slip faulting in the Aegean extensional province. *Tectonophysics* **391**, 67–83.

ROSI, M. 1992. A model for the formation of vesiculated tuff by the coalescence of accretionary lapilli. *Bulletin of Volcanology* **54**, 429–34.

SCHUMACHER, R. & SCHMINCKE, H.-U. 1995. Models for the origin of accretionary lapilli. *Bulletin of Volcanology* **56**, 626–39.

SELF, S. & SPARKS, R.S.J. 1978. Characteristics of widespread pyroclastic deposits formed by the interaction of silicic magma and water. *Bulletin of Volcanology* **41**, 196–212.

SHAUB, B.M. 1979. Genesis of thundereggs, geodes, and agates of igneous origin. *Lapidary Journal* **32**, 2340–66.

SMITH, V.C., SHANE, P. & NAIRN, I.A. 2005. Trends in rhyolite geochemistry, mineralogy, and magma storage during the last 50 kyr at Okataina and Taupo volcanic centres, Taupo Volcanic Zone, New Zealand. *Journal of Volcanology and Geothermal Research* **148**, 372–406.

SOHN, Y.K. & CHOUGH, S.K. 1989. Depositional processes of the Suwolbong tuff ring, Cheju Island (Korea). *Sedimentology* **36**, 837–55.

SOHN, Y.K. & PARK, K.H. 2005. Composite tuff ring/cone complexes in Jeju Island, Korea: possible consequences of substrate collapse and vent migration. *Journal of Volcanology and Geothermal Research* **141**, 157–75.

STEVENSON, R.J., BRIGGS, R.M. & HODDER, A.P.W. 1994. Physical volcanology and emplacement history of the Ben-Lomond rhyolite lava flow, Taupo Volcanic Center, New-Zealand. *New Zealand Journal of Geology and Geophysics* **37**(3), 345–58.

TAIT, M.A., CAS, R.A.F. & VIRAMONTE, J.G. 2009. The origin of an unusual tuff ring of perlitic rhyolite pyroclasts: the last explosive phase of the Ramadas Volcanic Centre, Andean Puna, Salta, NW Argentina. *Journal of Volcanology and Geothermal Research* **183**, 1–16.

TARCAN, G. & GEMICI, Ü. 2003. Water geochemistry of the Seferihisar geothermal area, İzmir, Turkey. *Journal of Volcanology and Geothermal Research* **126**, 225–42.

TÜRKELLI, N., KALAFAT, D. & GÜNDOĞDU, O. 1995. 6 Kasım 1992 İzmir (Doğanbeyli) depremi saha gözlemleri ve odak mekanizma çözümü. *Jeofizik* **9–10**, 343–8.

TÜRKELLI, N., KALAFAT, D. & İNCE, Ş. 1990. 6 Kasım 1992 İzmir depremi ve artçı şokları. *Deprem Araştırma Bülteni* **68**, 58–95.

UZEL, B. & SÖZBILIR, H. 2008. A first record of a strike-slip basin in Western Anatolia and its tectonic implication: the Cumaovası Basin. *Turkish Journal of Earth Sciences* **17**, 559–91.

WAITT, R.B. & DZURISIN, D. 1981. Proximal airfall deposits from the May 18 eruption: stratigraphy and field sedimentology. In: *The 1980 Eruptions of Mount St Helens, Washington* (LIPMAN, P.W. & MULLINEAUX, D.R., eds), 601–16. US Geological Survey Professional Paper, **1250**.

WOHLETZ., K.H. & SHERIDAN, M.F. 1979. A model of pyroclastic surge. In *Ash-flow Tuffs* (eds C.E. Chapin & W.E. Elston), pp. 177–94. Geological Society of America, Special Paper no. 180.

YAĞMURLU, F. 1980. Bornova (İzmir) güneyi fliş topluluklarının jeolojisi. *Bulletin of the Geological Society of Turkey* **23**, 141–52.